CHAPTER

Microphones

5

CHAPTER OUTLINE

Part XV: General characteristics of microphones 199
5.1 Pressure microphones 200
5.2 Pressure-gradient microphones 202
5.3 Combination pressure and pressure-gradient microphones 206
Part XVI: Pressure microphones 208
5.4 Electromagnetic moving-coil microphone (dynamic microphone) 208
5.5 Electrostatic microphone (capacitor microphone) 216
Part XVII: Pressure-Gradient microphones 225
5.6 Electromagnetic Ribbon microphones 225
Part XVIII: Combination microphones 228
5.7 Electrical combination of pressure and pressure-gradient transducers 228
5.8. Acoustical combination of pressure and pressure-gradient microphones 230
5.9. Dual-diaphragm combination of pressure and pressure-gradient microphones 231
Omni-directional performance 233
Bi-directional Performance 237
Uni-directional Performance 237
Condition for equal sensitivity in all three switch positions 238
Condition for Stability 239

PART XV: GENERAL CHARACTERISTICS OF MICROPHONES

Microphones are electroacoustic transducers for converting acoustic energy into electric energy. They serve two principal purposes. First, they are used for converting music or speech into electric signals which are transmitted or processed in some manner and then reproduced. Second, they serve as measuring instruments, converting acoustic signals into electric currents which are processed and displayed. In some applications like telephony, high electrical output, low cost, and durability are greater considerations than fidelity of reproduction. In other applications, small size and high fidelity are of greater importance than high sensitivity and low cost. In measurement applications we may be interested in determining the sound pressure or the particle velocity. In some applications the microphone must operate without appreciable change in characteristics regardless of major changes in temperature and barometric pressure.

Acoustics: Sound Fields and Transducers. DOI: 10.1016/B978-0-12-391421-7.00005-1

Table 5.1 Summary of different microphone types

Microphone type	Pressure	Pressure-gradient
Electrostatic: (condenser, electret, or piezoelectric)	Displacement-sensitive Stiffness-controlled High-frequency resonance	Velocity-sensitive Resistance-controlled Mid-frequency resonance
Electromagnetic: (moving-coil or ribbon)	Velocity-sensitive Resistance-controlled Mid-frequency resonance	Acceleration-sensitive Mass-controlled Low-frequency resonance

For these different applications, a variety of microphones have been developed. For purposes of discussion in this part they are divided into three broad classes in each of which there are a number of alternative constructions. The classes are:

Pressure microphones.
Pressure-gradient microphones.
Combinations of (1) and (2).

In this part we shall describe the distinguishing characteristics of these three types. In the next two parts we shall discuss in detail several examples of each type involving electromagnetic and electrostatic types of transduction. A brief summary of their characteristics is given in Table 5.1, which will be explained in greater detail during this chapter.

5.1 PRESSURE MICROPHONES

A pressure microphone is one that responds to changes in sound pressure. A common example of a pressure microphone is one with a diaphragm, the back side of which is terminated in a closed cavity (see Fig. 5.1). A tiny hole through the wall of the cavity keeps the average pressure inside of the cavity

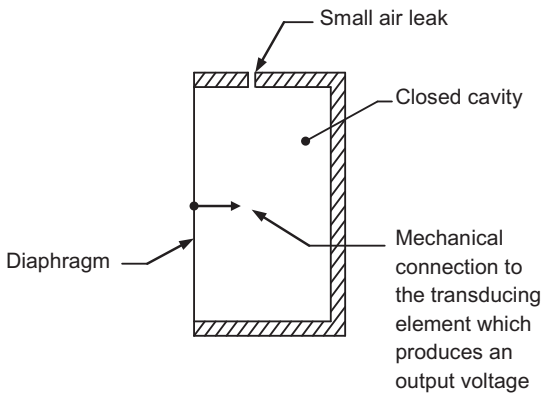

FIG. 5.1 Sketch of a pressure-actuated microphone consisting of a rigid enclosure, in one side of which there is a flexible diaphragm connected to a transducing element.

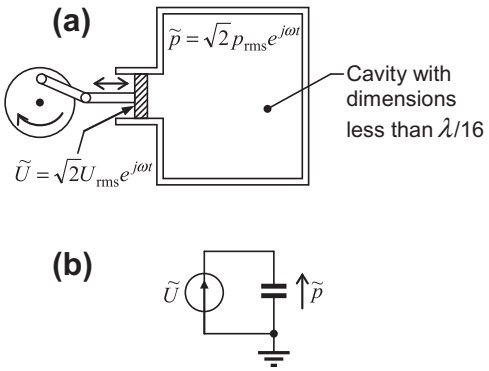

FIG. 5.2 Sketch of a pressure chamber.

at atmospheric pressure. However, rapid changes in pressure, such as those produced by a sound wave, cause the diaphragm to move backward and forward.

If a pressure microphone is placed in a small cavity in which the pressure is varied, as shown in Fig. 5.2, the output voltage will be the same regardless of what position the microphone occupies in the cavity. On the other hand, if a pressure microphone is placed at successive points 1, 2, 3, and 4 of Fig. 5.3a, it will respond differently at each of these points for reasons that can be seen from Fig. 5.3b. The pressure drops p_1, p_2, p_3, and p_4 are different from each other by an amount Δp, if the spacings Δx are alike.

If a pressure microphone is placed in a plane sound wave of constant intensity I (watts flowing through a unit area in the plane of the wave front), the force acting to move the diaphragm will be independent of frequency because $p_{rms} = \sqrt{I\rho_0 c}$ [see Eq. (1.12)].

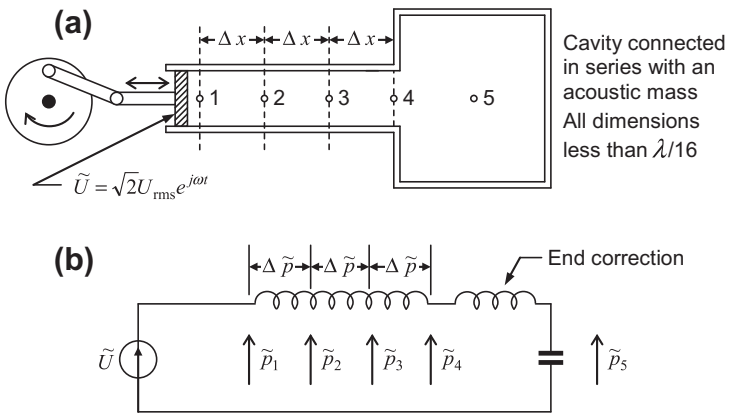

FIG. 5.3 Sketch of an arrangement in which a pressure gradient is produced.

5.2 PRESSURE-GRADIENT MICROPHONES

A pressure-gradient microphone is one that responds to a difference in pressure at two closely spaced points. A common example of this type of microphone has a diaphragm, both sides of which are exposed to the sound wave. Such a construction is shown in Fig. 5.4.

If a pressure-gradient microphone is placed in the cavity of Fig. 5.2a, there will be no net force acting on the diaphragm and its output will be zero. This happens because there is no pressure gradient in the cavity. In contrast, if a pressure-gradient microphone is placed at the successive positions 1 to 4 of Fig. 5.3a, it will produce an output voltage proportional to the pressure gradient $\Delta p/\Delta x$. in other words, if Δx is the same between successive points, the microphone output will be independent of whichever of the four positions it occupies in Fig. 5.3a.

If a very small pressure-gradient microphone is placed in a plane sound wave traveling in the x direction, the complex force $\tilde{f}_D$ acting to move the diaphragm will be

$$\tilde{f}_D = -S\frac{\partial \tilde{p}}{\partial x}\Delta l \cos\theta \tag{5.1}$$

where

$\tilde{p}$ is sound pressure
$\frac{\partial \tilde{p}}{\partial x}\cos\theta$ is the component of the x gradient of pressure acting across the faces of the diaphragm
θ is the angle the normal to the diaphragm makes with the direction of travel of the wave (see Fig. 5.5)
Δl is the effective distance between the two sides of the diaphragm (see Fig. 5.4)
S is area of diaphragm.

The equation for a plane traveling sound wave has already been given [Eq. (2.86)]; It is

$$\tilde{p} = \tilde{p}_0 e^{-jkx} \tag{5.2}$$

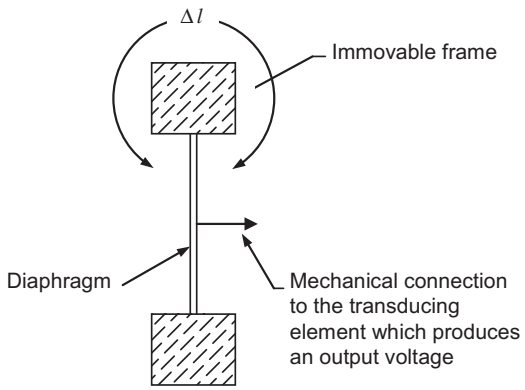

FIG. 5.4 Sketch of a pressure-gradient microphone consisting of a movable diaphragm, both sides exposed, connected to a transducing element.

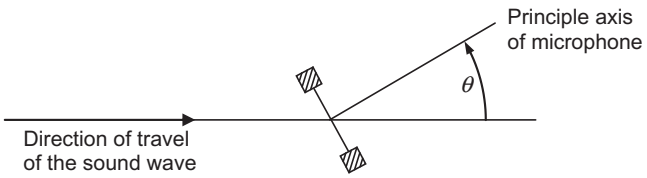

FIG. 5.5 Pressure-gradient microphone with principal axis located at an angle θ with respect to the direction of travel of the sound wave.

where

$k = \omega/c$
$\tilde{p}_0$ is pressure at $x = 0$

If we assume that the introduction of the microphone into the sound field does not affect the pressure gradient, we may substitute Eq. (5.2) into Eq. (5.1) and get

$$\tilde{f}_D = \frac{j\tilde{p}_0 \omega S\, \Delta l \cos\theta}{c} e^{-jkx} \tag{5.3}$$

The magnitude of the force at any point x is

$$\left|\tilde{f}_D\right| = \frac{\left|\tilde{p}\right| \omega S\, \Delta l \cos\theta}{c} \tag{5.4}$$

It should be remembered [see Eq. (2.4)] that in the steady state the pressure gradient is proportional to $j\omega\rho_0$ times the component of particle velocity in the direction the gradient is being taken. The force f_D is therefore proportional to the particle velocity at any given frequency. Reference to Fig. 5.5 is sufficient to convince one that when $\theta = 90°$, the force acting on the diaphragm will be zero, because conditions of symmetry require that the pressure be the same on both sides of the diaphragm. From Eq. (5.4) we also see that the effective force acting on the diaphragm is proportional to frequency and to the sound pressure.

In spherical coordinates, for a microphone whose dimensions are small compared with r, Eq. (5.1) becomes

$$\tilde{f}_D = -S \frac{\partial \tilde{p}}{\partial r} \Delta l \cos\theta \tag{5.5}$$

The equation for a spherical wave is found from Eq. (2.107).

$$\tilde{p}(r) = \tilde{A}_0 \frac{e^{-jkr}}{r} \tag{5.6}$$

Substituting (5.6) in (5.5) gives

$$\tilde{f}_D = \frac{\tilde{A}_0(1 + jkr)}{r^2} e^{-jkr} S(\Delta l \cos\theta) \tag{5.7}$$

This yields

$$\left|\tilde{f}_D\right|\text{rms} = \frac{\left|\tilde{p}\right|_{\text{rms}} \omega S\, \Delta l \cos\theta}{c} \cdot \frac{\sqrt{1+k^2r^2}}{kr} \tag{5.8}$$

However, we see from Eq. (2.89) that in a plane wave the rms velocity is related to the rms pressure by

$$\left|\tilde{u}\right|_{\text{rms}} = \frac{\left|\tilde{p}\right|_{\text{rms}}}{\rho_0 c} \tag{5.9}$$

and in a spherical wave [Eq. (2.109)]

$$\left|\tilde{u}\right|_{\text{rms}} = \frac{\left|\tilde{p}\right|_{\text{rms}}}{\rho_0 c} \frac{\sqrt{1+k^2r^2}}{kr} \tag{5.10}$$

where $|\tilde{u}|_{\text{rms}}$ is the rms particle velocity in the direction of travel of the sound wave. Hence, Eqs. (5.4) and (5.8) become

$$\left|\tilde{f}_D\right|_{\text{rms}} = \left|\tilde{u}\right|_{\text{rms}} \omega \rho_0 S\, \Delta l \cos\theta \tag{5.11}$$

In other words, the effective (rms) force f_D acting on the diaphragm of a pressure-gradient microphone is directly proportional to the effective particle velocity in the direction of propagation of the wave, to the frequency, to the density of the air, to the size and area of the diaphragm, and to the angle it makes with the direction of propagation of the sound wave. This statement is true for any type of wave front—plane, spherical, cylindrical, or other—provided the microphone is so small that its presence does not appreciably disturb the sound wave.

At any given frequency, the response of the microphone is proportional to the $\cos\theta$, which yields the *directivity pattern* shown in Fig. 5.6a. This shape of plot is commonly referred to as a "figure of 8" pattern. The same pattern, plotted in decibels relative to the force at $\theta = 0$, is given in (b). It is interesting to observe that the pattern is the same as that for an acoustic doublet or for an unflanged diaphragm at low frequencies (see Fig. 4.23 and Fig. 13.23).

The frequency response of a pressure-gradient (particle-velocity) microphone, when placed in a spherical wave, is a function of the curvature of the wave front. That is to say, from Eq. (5.10) we see that for values of k^2r^2 (kr equals $\omega r/c$) large compared with 1 the particle velocity is linearly related to the sound pressure. A large value of kr means that either the frequency is high or the radius of curvature of the wave front is large. However, for values of k^2r^2 small compared with 1, which means that the radius of curvature is small or the frequency is low, or both, the particle velocity is proportional to $|\tilde{p}|/(\omega r)$. As a result, when a person talking or singing moves near to a pressure-gradient microphone so that r is small his voice seems to become more "boomy" or "bassy" because the output of the microphone increases with decreasing frequency.

The path difference Δl depends on whether the diaphragm is a rigid piston or flexible. Since a microphone may be considered to be a sound source in reverse, we can use the radiation impedance

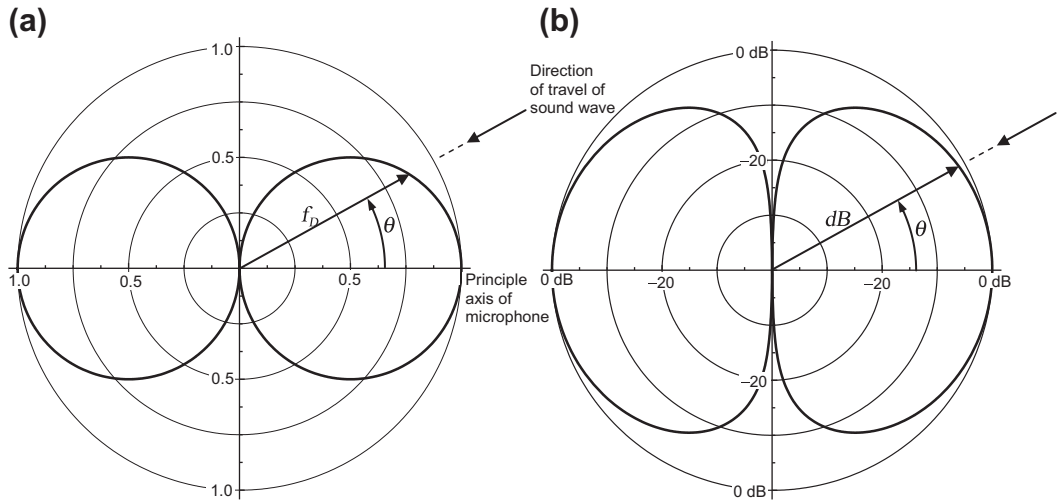

FIG. 5.6 (a) Directivity characteristic of the pressure-gradient microphone of Fig. 5.4. (b) Same but with scale in dB.

of the equivalent rigid or flexible sound source to give us the relationship between the diaphragm pressure and velocity in Eqs. (5.1) and (5.11), which are rearranged thus

$$Z_s = \frac{\tilde{f}_D}{S\tilde{u}} = j\omega\rho_0 \, \Delta l \cos\theta, \tag{5.12}$$

so that we can solve for Δl. We will assume that the incident sound waves are on axis so that $\theta = 0$. In the case of a rigid circular piston of radius a with no baffle, the specific radiation impedance Z_s is given by

$$Z_s\big|_{\lambda>>a} = \frac{\tilde{f}_D}{S\tilde{u}} = j\rho_0 c \frac{4ka}{3\pi}. \tag{5.13}$$

Equating Eqs. (5.12) and (5.13) yields

$$\Delta l = \frac{4a}{3\pi}. \tag{5.14}$$

Using the resilient disk in free space model to give the radiation impedance for a perfectly flexible diaphragm, where

$$Z_s\big|_{\lambda>>a} = j\rho_0 c\pi ka/4,$$

we find that

$$\Delta l = \frac{\pi a}{4}. \tag{5.15}$$

5.3 COMBINATION PRESSURE AND PRESSURE-GRADIENT MICROPHONES

A combination pressure and pressure-gradient microphone is one that responds to both the pressure and the pressure gradient in a wave. A common example of such a microphone is one having a cavity at the back side of the diaphragm that has an opening to the outside air containing an acoustic resistance (see Fig. 5.7a).

The analogous circuit for this device is shown in Fig. 5.7b. If we let

$$\tilde{p}_1 = \tilde{p}_0 e^{-jkx} \tag{5.16}$$

$$\begin{aligned} \tilde{p}_2 &= \tilde{p}_1 + \frac{\partial\left(\tilde{p}_0 e^{-jkx}\right)}{\partial x}\Delta l \cos\theta \\ &= \tilde{p}_1\left(1 - j\frac{\omega}{c}\Delta l \cos\theta\right) \end{aligned} \tag{5.17}$$

Let us say that $\tilde{U}_D$ is the volume velocity of the diaphragm; $\tilde{U}_0$ is the volume velocity of the air passing through the resistance; $\tilde{p}_D$ is the net pressure acting to move the diaphragm, and Z_{AD} is the diaphragm

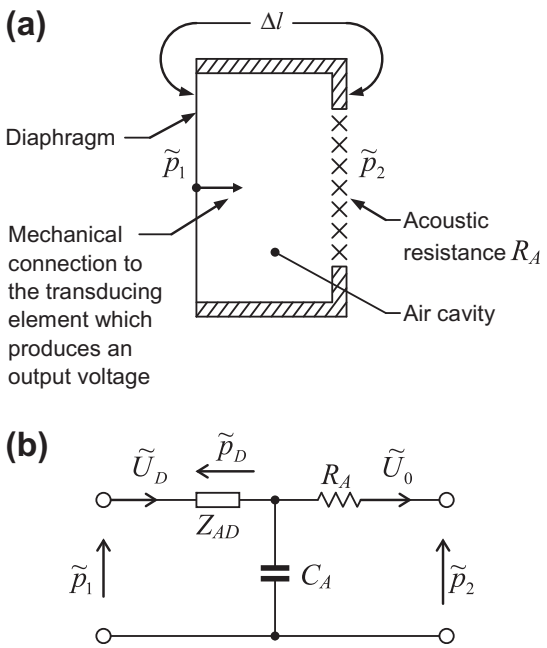

FIG. 5.7 (a) Sketch of a combination pressure and pressure-gradient microphone consisting of a right enclosure in one side of which is a movable diaphragm connected to a transducing element and in another side of which is an opening with an acoustic resistance R_A. (b) Acoustic-impedance circuit for (a).

impedance. In the case of an electrostatic or ribbon microphone, the radiation mass will have a significant effect, so for the sake of simplicity let us lump this in with Z_D. The acoustic resistance R_A will also have a mass component, but we assume that it is very small compared to the resistance. Then we can write the following equations from Fig. 5.7b:

$$\begin{aligned} \tilde{U}_D\left(Z_{AD}+\frac{1}{j\omega C_A}\right)-\frac{\tilde{U}_0}{j\omega C_A} &= \tilde{p}_1 \\ -\frac{\tilde{U}_D}{j\omega C_A}+\tilde{U}_0\left(R_A+\frac{1}{j\omega C_A}\right) &= -\tilde{p}_2, \end{aligned} \tag{5.18}$$

which are solved for $\tilde{U}_D$. The pressure difference across the diaphragm is

$$\tilde{p}_D = \tilde{U}_D Z_{AD} = \frac{Z_{AD}\left(\tilde{p}_1 R_A+\dfrac{\tilde{p}_1-\tilde{p}_2}{j\omega C_A}\right)}{Z_{AD}R_A - j((R_A+Z_{AD})/\omega C_A)} \tag{5.19}$$

Substitution of (5.17) in (5.19) yields

$$\tilde{p}_D = \tilde{p}_1 \frac{Z_{AD}\left(R_A+\dfrac{\Delta l\cos\theta}{cC_A}\right)}{Z_{AD}R_A - j((R_A+Z_{AD})/\omega C_A)} \tag{5.20}$$

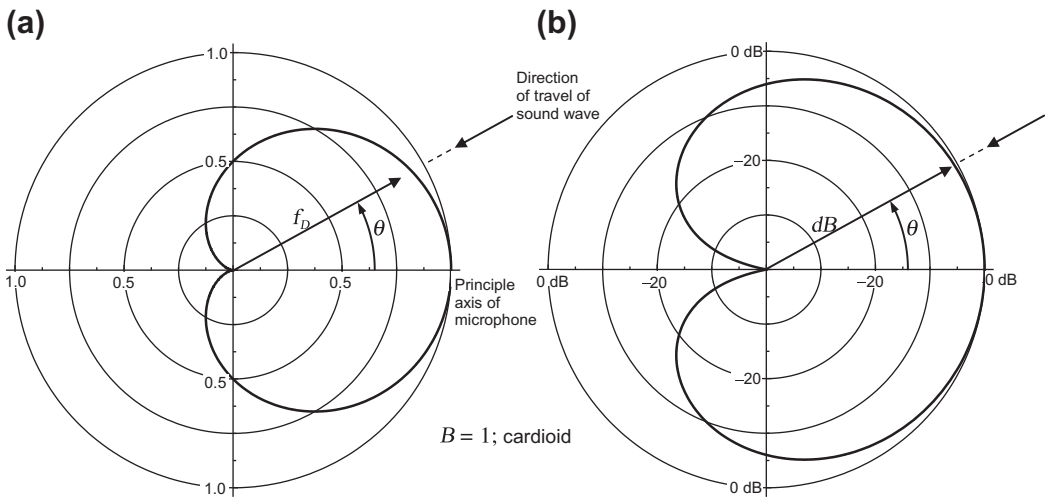

FIG. 5.8 (a) Directivity characteristic of the combination pressure and pressure-gradient microphone of Fig. 5.7. (b) Same but with scale in dB.

Let

$$\frac{\Delta l}{cC_A R_A} = B \tag{5.21}$$

where B is an arbitrarily chosen dimensionless constant. Since $\tilde{f}_D = \tilde{p}_D S$, where S is the effective area of the diaphragm, we have

$$\left|\tilde{f}_D\right| = \tilde{p}_1 \, |A| \, S(1 + B\cos\theta) \tag{5.22}$$

where A is the ratio

$$A = \frac{Z_{AD} R_A}{Z_{AD} R_A - j((R_A + Z_{AD})/\omega C_A)} \tag{5.23}$$

A plot of the force $|f_D|$ acting on the diaphragm as a function of θ for $B = 1$ is shown in Fig. 5.8a. The same pattern plotted in decibels is given in (b). The *directivity pattern* for $B = 1$ is commonly called a *cardioid pattern*. Other directivity patterns are shown in Fig. 5.30 for B = 0, $\frac{1}{2}$, 1, $\sqrt{3}$, 3 and ∞.

PART XVI: PRESSURE MICROPHONES

Pressure microphones are the most widely used of the three basic types discussed in the preceding part. They are applicable to acoustic measuring systems and to the pickup of music and speech in broadcast studios, in public-address installations, and in hearing aids. Many engineers and artists believe that music reproduced from the output of a well-designed pressure microphone is superior to that from the more directional types of microphone because the quality of the reverberation in the auditorium or studio is fully preserved, because undesirable wave-form distortion is minimized, and because the quality of the reproduced sound is not as strongly dependent as for other types upon how close the talker or the musical instrument is to the microphone.

Two principal types of pressure microphones are commonly found in broadcasting, public address, recording, and acoustical measurement. They are the electromagnetic and electrostatic types. We shall analyze one commercially available microphone of each of these two types in the next few sections of this part. Various other types of microphones are used in other applications, such as the piezoelectric hydrophone in underwater systems, the hot-wire microphone in aerodynamic measurements, and the Rayleigh disk in absolute particle-velocity measurements. Lack of space precludes their inclusion here. However, electret (electrostatic with stored charge) and MEMS (micromechanical) types will be discussed in Chapter 8 in relation to cellphones.

5.4 ELECTROMAGNETIC MOVING-COIL MICROPHONE (DYNAMIC MICROPHONE)

General features. The moving-coil electromagnetic microphone is a medium-priced instrument of high sensitivity. It is principally used in broadcast work and in applications where long cables are required or where rapid fluctuations or extremes in temperature and humidity are expected.

The best designed moving-coil microphones have open-circuit voltage responses to sounds of random incidence that are within 5 dB of the average response over the frequency range between 40 and 16000 Hz. Sound pressures as low as 16 dB SPL and as high as 140 dB SPL re 20 μPa can be measured. Changes of response with temperature, pressure, and humidity are believed to be, in the better instruments, of the order of 3 to 5 dB maximum below 1000 Hz for the temperature range of 10 to 100°F, pressure range of 0.65 to 0.78 m Hg, and humidity range of 0 to 90 per cent relative humidity.

The electrical impedance is that of a coil of wire. Below 1000 Hz, the resistive component predominates over the reactive component. Most moving-coil microphones have a nominal electrical impedance of about 300 Ω. The mechanical impedance is not high enough to permit use in a closed cavity without seriously changing the sound pressure therein.

To connect a dynamic microphone to an amplifier, a stepping-up transformer is required, which is usually contained within the microphone housing.

Construction. The electromagnetic moving-coil microphone consists of a diaphragm that has fastened to it a coil of wire situated in a magnetic field (see Fig. 5.9a). In addition, there are acoustical circuits behind and in front of the diaphragm to extend the response of the microphone over a greater frequency range. A cut-away view of a widely used type of moving-coil microphone is shown in Fig. 5.9b and a cross-sectional sketch is shown in Fig. 5.10.

Electro-mechano-acoustical relations. The sound passes through the dust screen and arrives at an array of sound holes in front of the diaphragm, which form a small acoustic mass and a small acoustic resistance, although most of the acoustic resistance is provided by the dust screen. The holes are so

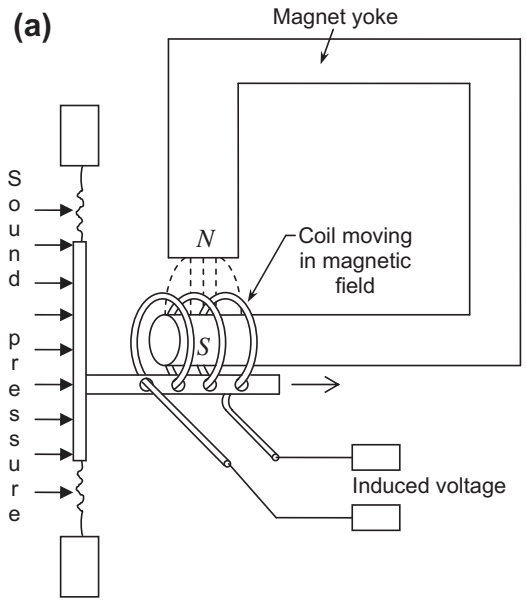

FIG. 5.9 (a) Diagrammatic representation of the essential elements of a moving-coil (dynamic) microphone.

From Beranek, Acoustic Measurements, *John Wiley & Sons, Inc., New York, 1949.*

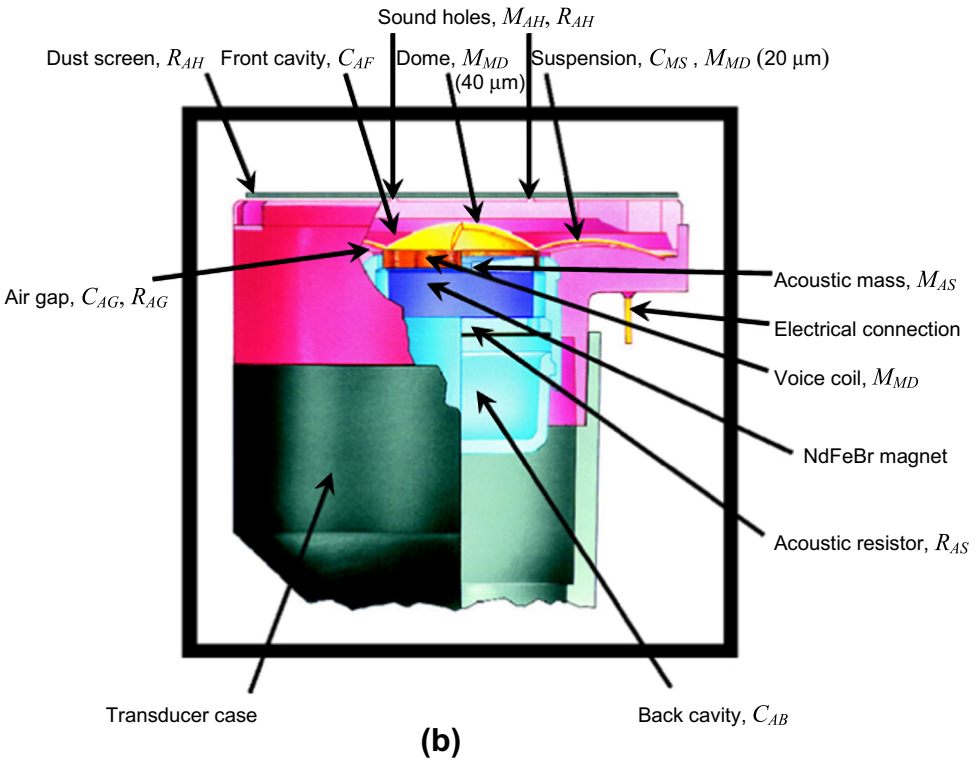

FIG. 5.9 (b) Cutaway view of a commercially available moving-coil microphone type D230.

In this varimotion™ design, the thickness of the diaphragm varies radially in order to provide higher compliance in the suspension and greater stiffness at the center, which moves the dome break-up modes out of the operating frequency range.

Courtesy of AKG.

small that their radiation impedance, operating as a loudspeaker, is essentially reactive over the whole frequency range (see Fig. 4.39). The front cavity between the holes and diaphragm is a small acoustic compliance. Hence, the total acoustical circuit *in front of the diaphragm* is that of Fig. 5.11. The pressure $\tilde{p}_B$ is that which the sound wave would produce at the faces of the holes if they were closed off. $\tilde{U}_H$ is the volume velocity of the air that moves through the holes. $\tilde{U}_D$ is the volume velocity of the diaphragm and is equal to the effective linear velocity $\tilde{u}_D$ of the diaphragm times its effective area S_D. The radiation mass looking outward from the grid openings is M_{AA}. The acoustic mass and resistance of the holes and dust screen are M_{AH} and R_{AH}. The compliance of the air space in front of the diaphragm is C_{AF}. At all frequencies, except the very highest, the effect of the protective screen can be neglected.

Behind the diaphragm the acoustical circuit is more complicated. First there is an air gap between the diaphragm and the magnet that forms an acoustic compliance and resistance (see Fig. 5.9b). This air gap connects with a large back cavity that is also an acoustic compliance. In the connecting

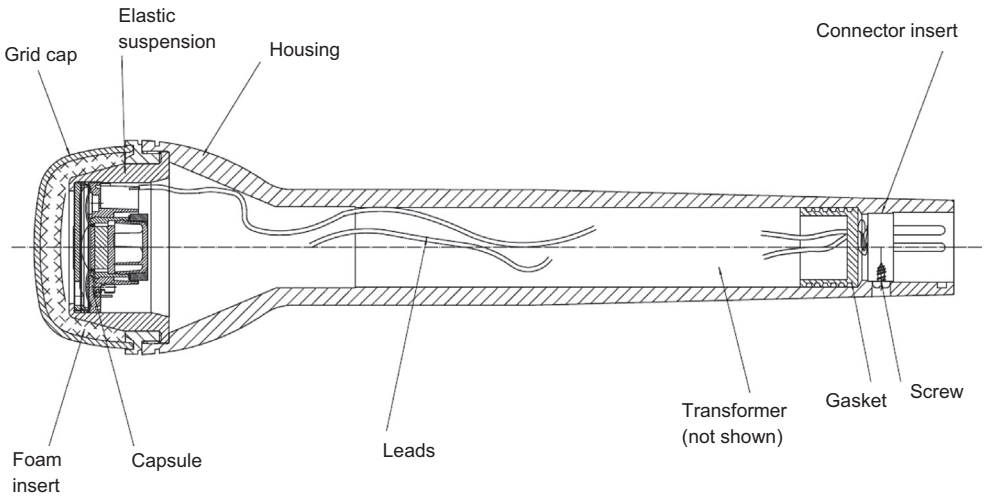

FIG. 5.10 Cross-section of a commercially available moving-coil microphone type D230.

Courtesy of AKG.

passages there are screens that serve as acoustic resistances. Also, the interconnecting passages form an acoustic mass. The large air cavity connects to the outside of the microphone through a narrow pressure-equalizing tube, which prevents static displacements of the diaphragm due to variations in atmospheric pressure. It also attenuates the output of the microphone at the very lowest frequencies because the sound arriving at the rear of the diaphragm via the tube cancels that at the front. However, for simplicity, we shall ignore this tube during our analysis because its effect is only evident well below the working frequency range of the microphone, although in some designs it is tuned to resonate with the back cavity and thus boost the low frequency output rather like a bass-reflex port in a loudspeaker, a topic which is covered in more detail in Chapter 6.

The complete acoustical circuit behind the diaphragm is given in Fig. 5.12. The acoustic compliance and resistance directly behind the diaphragm are C_{AG} and R_{AG} respectively, the acoustic resistances of the screens are R_{AS}, the acoustic mass of the inter-connecting passage is M_{AS}, and the acoustic compliance of the large back cavity is C_{AB}.

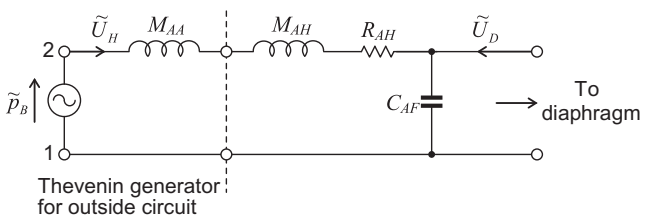

FIG. 5.11 Acoustical circuit for the elements in front of the diaphragm of the microphone of Fig. 5.9 (acoustic-impedance analogy).

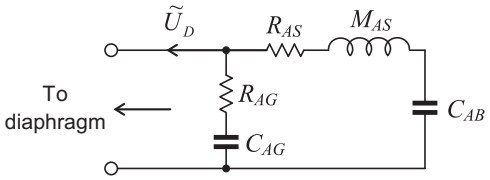

FIG. 5.12 Acoustical circuit for the elements behind the diaphragm of the microphone of Fig. 5.9 (acoustic-impedance analogy).

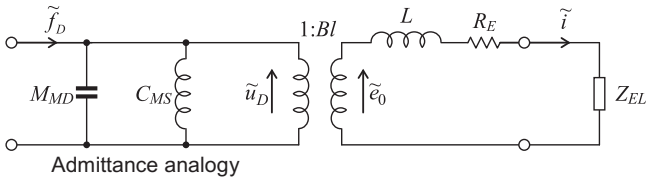

FIG. 5.13 Mechano-electrical circuit of diaphragm, voice coil, and magnetic field of the microphone of Fig. 5.9 (mechanical-admittance analogy).

The electromechanical circuit (mechanical-admittance analogy) for the diaphragm and voice coil is given in Fig. 5.13. The force exerted on the diaphragm is $\tilde{f}_D$, and its resulting velocity is $\tilde{u}_D$. Here, M_{MD} = mass of diaphragm and voice coil; C_{MS} = compliance of the suspension; L = inductance of voice coil; and R_E electric resistance of the voice coil. Z_{EL} is the electric impedance of the electric load to which the microphone is connected. The quantity $\tilde{e}_0 = Bl\tilde{u}_D$ is the open-circuit voltage produced by the microphone. There will also be some mechanical resistance due to the suspension, but this is generally very small compared to the acoustic resistance R_{AS} so we will ignore it.

In order to combine Fig. 5.11, Fig. 5.12, and Fig. 5.13, the dual of Fig. 5.13 must first be taken; it is shown in Fig. 5.14. Now, in order to join Fig. 5.11, Fig. 5.12, and Fig. 5.14, all forces in Fig. 5.14 must be divided by the area of the diaphragm S_D and all velocities multiplied by S_D. This can be done by inserting an area transformer into the circuit. Recognizing that $\tilde{U}_D$ must be the same for all three component circuits, we get the circuit of Fig. 5.15 for the moving-coil microphone.

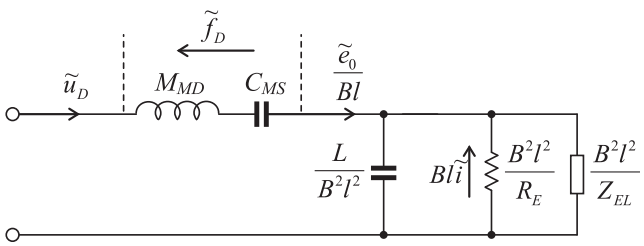

FIG. 5.14 Mechano-electrical circuit of the diaphragm, voice coil, and magnetic field of the microphone of Fig. 5.9 (mechanical-impedance analogy).

Note that u_D is also equal to e_0/Bl.

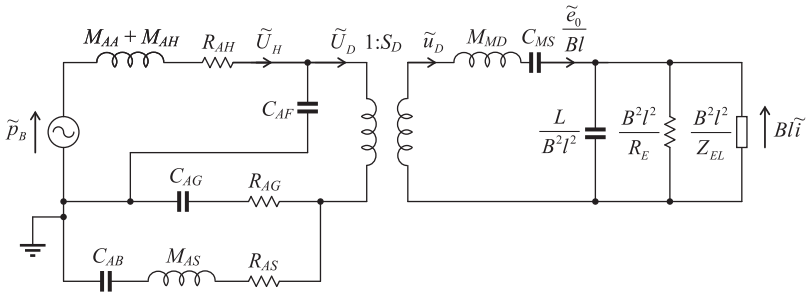

FIG. 5.15 Complete electro-mechano-acoustical circuit of the moving-coil microphone of Fig. 5.9 (impedance analogy).

The electromechanical transformer has been cleared from the circuit.

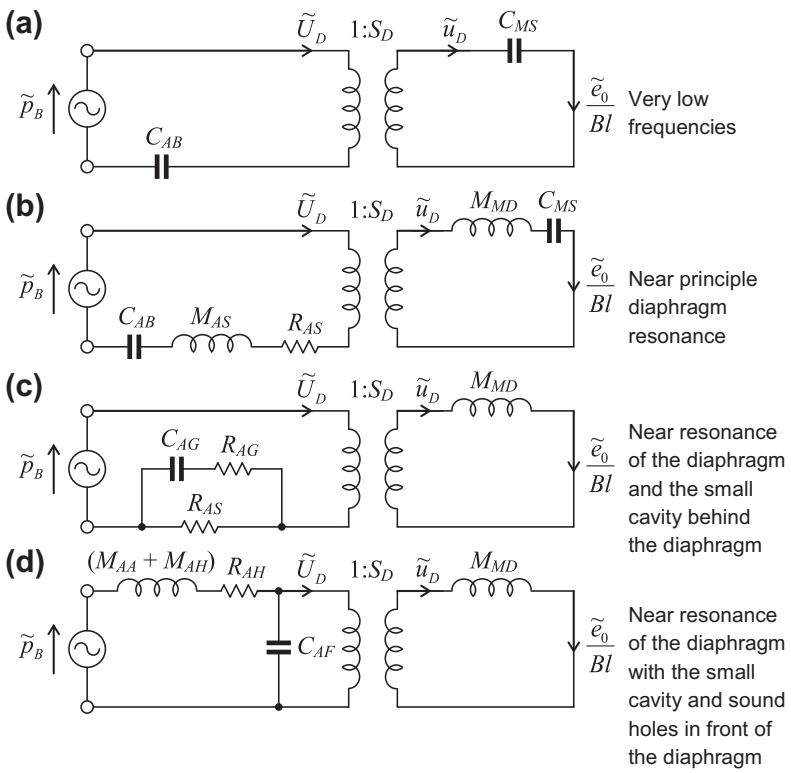

FIG. 5.16 Moving-coil microphones. Simplified circuits for four frequency regions (impedance analogy).

The excess pressure produced by the sound wave at the front of the microphone with the sound holes blocked off is $\tilde{p}_B$ and the open-circuit voltage is $\tilde{e}_0$.

Performance. The performance of the circuit of Fig. 5.15 can best be understood by reference to Fig. 5.16, which is derived from Fig. 5.15. Let us assume from now on that $Z_{EL} \rightarrow \infty$. This means that the electrical terminals are open-circuited so that the voltage appearing across them is the open-circuit voltage $\tilde{e}_0$ (see Fig. 5.13). In the circuit of Fig. 5.15, the "short-circuit" velocity is equal to $\tilde{e}_0/Bl$.

At very low frequencies Fig. 5.15 reduces to Fig. 5.16a. The generator $\tilde{p}_B$ is effectively open-circuited by the three acoustic compliances C_{AF}, C_{AG}, and C_{AB}, and the mechanical compliance C_{MS} of which only C_{AB} and C_{MS} have appreciable size. Also, all of the resistances and reactances of the masses are small compared with the reactances of C_{AB} and $C_{MS}S_D^2$. Hence, $\tilde{e}_0$ is very small. This region is marked (a) in Fig. 5.17, where we see the voltage response in decibels as a function of frequency. In region (a) the response increases at the rate of 6 dB per octave increase in frequency.

As the frequency increases (see Fig. 5.16b), a highly damped resonance condition occurs involving the resistance and mass of the screens behind the diaphragm, R_{AS} and M_{AS}, and the diaphragm constants themselves, M_{MD} and C_{MS}., together with the compliance C_{AB} back of the back cavity. This is region (b) of Fig. 5.17. A highly important design feature, therefore, is a resistance of the screens R_{AS} large enough so that the response curve in region (b) is as flat as possible. The damping is so great that it makes more sense to define this region by two break frequencies ω_L and ω_U, which define the upper and lower limits of this region rather than a single resonance frequency ω_0. These are defined by

$$\omega_L = \frac{C_{AB} + S_D^2 C_{MS}}{R_{AS} C_{AB} S_D^2 C_{MS}} \tag{5.24}$$

$$\omega_U = \frac{R_{AS}}{M_{AS} + M_{MD}/S_D^2} \tag{5.25}$$

and

$$\omega_0 = \sqrt{\omega_L \omega_U} \tag{5.26}$$

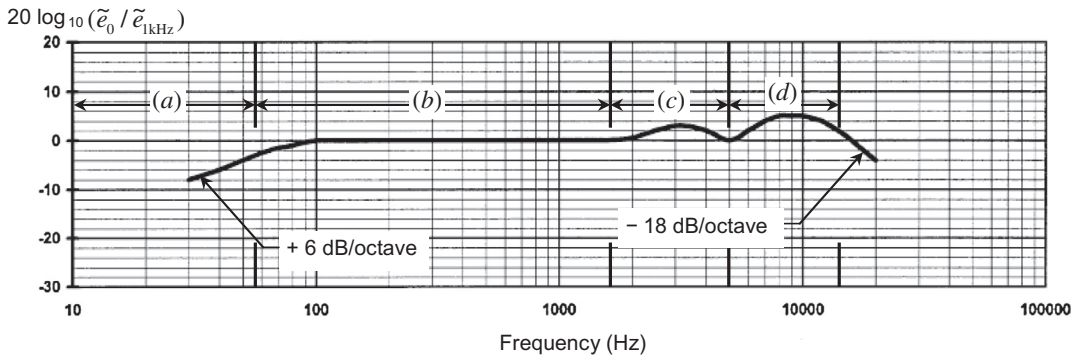

FIG. 5.17 Open-circuit-voltage response characteristic of a moving-coil microphone of the type shown in Fig. 5.9.

The vertical scale is in dB and the reference voltage $\tilde{e}_{1\text{kHz}}$ is the value of $\tilde{e}_0$ at 1 kHz.

Courtesy of AKG

The lower frequency ω_L marks the beginning of the 6 dB/octave low-frequency roll-off, which occurs at 55 Hz in Fig. 5.17, where the response is 3 dB less than that in the flat region. The upper frequency ω_U occurs somewhere near the upper limit of region (*b*). At the resonance frequency ω_0, the mass and compliance elements cancel each other's reactances leaving just resistive element R_{AS}. At this frequency, the mid-band sensitivity is given by

$$\tilde{e}_0 = \frac{Bl\tilde{p}_B}{S_D R_{AS}} \tag{5.27}$$

In the case of the microphone shown in Fig. 5.9, the sensitivity is 2.4 mV/Pa or − 52 dBV/Pa.

Above region (*b*) (see Fig. 5.16c), a resonance condition results that involves primarily the mass of the diaphragm M_{MD} and the stiffness of the air immediately behind it, C_{AG}. This yields the response shown in region (*c*) of Fig. 5.17. The resonance frequency ω_C at the center of region (*c*) is given by

$$\omega_C = \frac{S_D}{\sqrt{M_{MD} C_{AG}}} \tag{5.28}$$

Because the air gap is so small, the viscous air flow therein has a damping effect on this resonance, as represented by R_{AG} which is important for keeping the frequency response reasonably flat. The large value of R_{AS} damps the anti-resonance of C_{AG} with M_{AS}, which would otherwise produce a suck-out in the frequency response.

Finally, a third resonance occurs involving primarily the acoustical elements in front of the diaphragm [see Fig. 5.16d and region (*d*) of Fig. 5.17]. The resonance frequency ω_D at the center of region (*d*) is given by

$$\omega_D = \frac{1}{\sqrt{(M_{AA} + M_{AH}) C_{AF}}} \tag{5.29}$$

Because there are three reactive elements in the circuit ($M_{AA} + M_{AH}$, C_{AF}, and M_{MD}), the response then drops off at the rate of − 18 dB per doubling of frequency. Of course, this is the open-circuit roll-off and a steeper rate is likely to occur if the microphone is loaded with a capacitive cable which will resonate with the coil inductance at some frequency. A step-up transformer also has a limited bandwidth, although through careful design this need not compromise the performance of the microphone. The low-frequency response depends upon the inductance, which is maximized through use of a generous core size and an ample number of turns. The high-frequency response is extended through the use of a split bobbin in order to reduce the inter-winding capacitance and interleaving several primary and secondary sections, which reduces the leakage inductance.

These various resonance conditions result in a microphone whose response is substantially flat from 50 to 20000 Hz except for diffraction effects around the microphone. These diffraction effects will influence the response in different ways, depending on the direction of travel of the sound wave relative to the position of the microphone. The usual effect is that the response is enhanced in regions (*c*) and (*d*) if the sound wave impinges on the front of the microphone at normal (perpendicular) incidence compared with grazing incidence. One purpose of the outer protective screen is to minimize this enhancement.

5.5 ELECTROSTATIC MICROPHONE (CAPACITOR MICROPHONE)

General features. The electrostatic type of microphone is used extensively as a standard microphone for the measurement of sound pressure and as a studio microphone for the high-fidelity pickup of music. It can be made small in size so it does not disturb the sound field appreciably in the frequency region below 1000 Hz.

Sound-pressure levels as low as 10 dB and as high as 185 dB re 0.0002 microbar can be measured with standard instruments. The mechanical impedance of the diaphragm is that of a stiffness and is high enough so that measurement of sound pressures in cavities is possible. The electrical impedance is that of a pure capacitance.

The temperature coefficient for a well-designed capacitor microphone is less than 0.025 dB for each degree Celsius rise in temperature.

Continued operation at high relative humidities may give rise to noisy operation because of leakage across the insulators inside. Quiet operation can be restored by desiccation.

Construction. In principle, the electrostatic microphone consists of a thin diaphragm, a very small distance behind which there is a back plate (see Fig. 5.18). The diaphragm and back plate are electrically insulated from each other and form an electric capacitor. In precision measuring-microphones, commonly used diaphragm materials are nickel, stainless alloy, and titanium. Sometimes there can be problems with pin-holes in nickel and wrinkles in stainless alloy. Titanium suffers from neither of these problems. The thickness of the diaphragm is typically a few micrometers and the tension is usually greater than 2000 N/m.

A commercial form of this type of microphone is shown in Fig. 5.19. The holes in the back plate form an acoustic resistance that serves to damp the diaphragm at resonance. One manner in which the

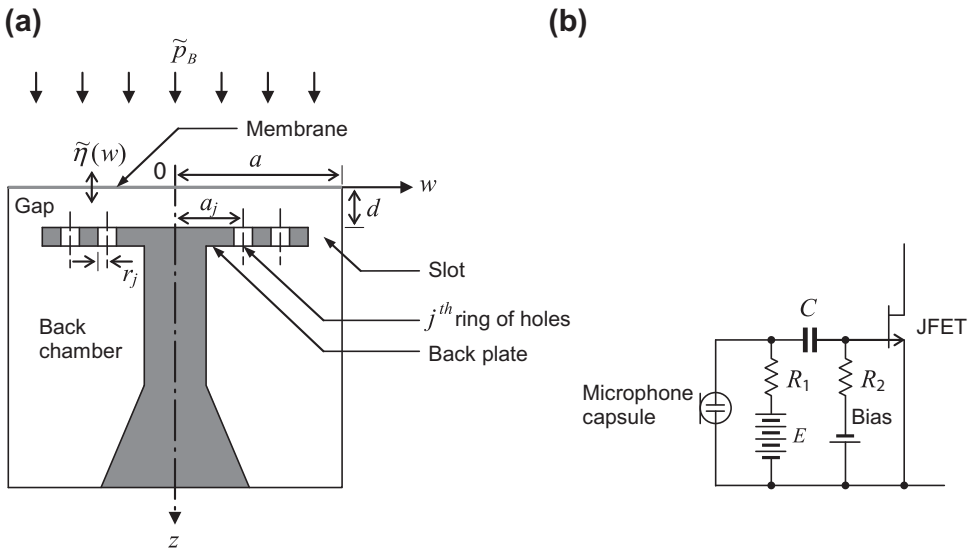

FIG. 5.18 (a) Cross-sectional sketch of an electrostatic microphone. (b) Simple FET circuit for use with capacitor microphone.

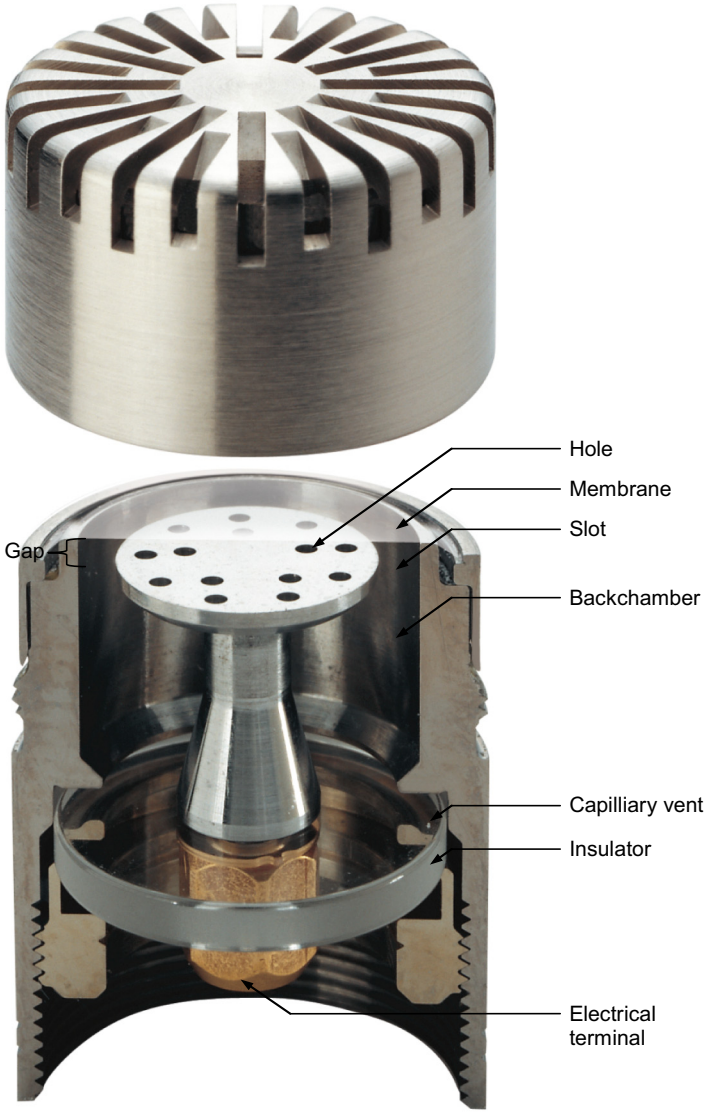

FIG. 5.19 Cutaway view of the B&K type 4190 capacitor microphone.

The perforated back plate serves both as the second terminal of the condenser and as a means for damping the principal resonant mode of the diaphragm. The cap with holes in it serves both for protection and as an acoustic network at high frequencies. This microphone has a polarizing voltage of $E = 200$ V.

Courtesy of Brüel & Kjær Sound & Vibration Measurement A/S.

microphones are operated is shown in Fig. 5.18b. The resistances R_1 and R_2 are made very large in order to keep the membrane charge constant at low frequencies and thus preserve the bass response. The direct voltage E is several hundred volts and acts to polarize the microphone. A JFET buffer amplifier is usually located close to the microphone capsule otherwise the capacitance of the microphone leads would exceed that of the microphone itself and therefore attenuate its output.

Electromechanical relations. Electrically, the electrostatic microphone is a capacitor with a capacitance that varies with time so that the total charge $Q(t)$ is

$$Q(t) = q_0 + q(t) = C_E(t)(E + e(t)) \tag{5.30}$$

where q_0 is the quiescent charge in coulombs, $q(t)$ is the incremental charge in coulombs, $C_E(t)$ is the capacitance in farads, E is the quiescent polarizing voltage in volts, and $e(t)$ is the incremental voltage in volts.

The capacitance $C_E(t)$ in farads is equal to (see Fig. 5.18*a*)

$$\begin{aligned} C_E(t) &= C_{E0} + C_{E1}(t) = \frac{\varepsilon_0 S}{d - \eta(t)} \approx \frac{\varepsilon_0 S}{d}\left(1 + \frac{\eta(t)}{d}\right) \\ &\approx C_{E0}\left(1 + \frac{\eta(t)}{d}\right) \end{aligned} \tag{5.31}$$

where C_{E0} is the capacitance in farads for $\eta(t) = 0$ and $C_{E1}(t)$ is the incremental capacitance in farads, ε_0 is a factor of proportionality that for air equals 8.85×10^{-12}, S is the effective area of one of the plates in square meters, d is the quiescent separation in meters, and $\eta(t)$ is the average incremental separation in meters. It is assumed in writing the right-hand term of Eq. (5.31) that the square of the maximum value of $\eta(t)$ is small compared with d^2.

If we similarly assumed that $[e(t)]^2_{\max} << E^2$, then Eqs. (5.30) and (5.31) yield

$$q_0 + q(t) = C_{E0}E + C_{E0}E\left(\frac{e(t)}{E} + \frac{\eta(t)}{d}\right) \tag{5.32}$$

so that

$$q(t) = C_{E0}\left(e(t) + \frac{E}{d}\eta(t)\right) \tag{5.33}$$

The total stored potential energy $W(t)$ at any instant is equal to the sum of the stored electrical and mechanical energies,

$$\frac{1}{2}Q(t)^2/C_E(t) \text{plus } \frac{1}{2}\eta(t)^2/C_{MS},$$

where C_{MS} is the mechanical compliance of the moving plate in m/N. That is,

$$\begin{aligned} W(t) &= \frac{1}{2}\frac{(q_0 + q(t))^2}{C_{E0} + C_{E1}(t)} + \frac{1}{2}\frac{\eta(t)^2}{C_{MS}} \approx \frac{1}{2}\frac{q_0^2 + 2q_0 q(t)}{C_{E0}\left(1 + \frac{\eta(t)}{d}\right)} \\ &+ \frac{1}{2}\frac{\eta(t)^2}{C_{MS}} = \frac{1}{2}\frac{q_0}{C_{E0}}(q_0 + 2q(t))\left(1 - \frac{\eta(t)}{d}\right) + \frac{1}{2}\frac{\eta(t)^2}{C_{MS}} \end{aligned} \tag{5.34}$$

The force in N at any instant acting to move the plate is, from the equation for work, $dW = f\,d\eta$,

$$f_0 + f(t) = \frac{dW(t)}{d\eta} \tag{5.35}$$

so that, by differentiation of Eq. (5.34),

$$\begin{aligned} f_0 + f(t) &\approx -\frac{q_0}{2dC_{E0}}(q_0 + 2q(t)) + \frac{\eta(t)}{C_{MS}} \\ &= -\frac{q_0^2}{2dC_{E0}} + \left(\frac{\eta(t)}{C_{MS}} - \frac{q(t)q_0}{dC_{E0}}\right) \end{aligned} \tag{5.36}$$

Hence, because $E = q_0/C_{E0}$,

$$f(t) = \frac{\eta(t)}{C_{MS}} - \frac{Eq(t)}{d} \tag{5.37}$$

Rearranging Eq. (5.33) gives

$$e(t) \approx -\frac{E\eta(t)}{d} + \frac{q(t)}{C_{E0}} \tag{5.38}$$

In the steady state,

$$\begin{aligned} j\omega\,\tilde{q} &= \tilde{i} \\ j\omega\,\tilde{\eta} &= \tilde{u} \end{aligned} \tag{5.39}$$

where $\tilde{q}$, $\tilde{i}$, $\tilde{\eta}$, and $\tilde{u}$ are now taken to be complex harmonically-varying quantities; so Eqs. (5.37) and (5.38) become, in z-parameter matrix form,

$$\begin{bmatrix} \tilde{f} \\ \tilde{e} \end{bmatrix} = \begin{bmatrix} \dfrac{1}{j\omega\,C_{MS}} & \dfrac{E}{j\omega\,d} \\ \dfrac{E}{j\omega\,d} & \dfrac{1}{j\omega\,C_{E0}} \end{bmatrix} \cdot \begin{bmatrix} \tilde{u} \\ -\tilde{i} \end{bmatrix} \tag{5.40}$$

with $\tilde{e}$ and $\tilde{f}$ also being complex harmonically-varying quantities.

Analogous circuits. Equation (5.40) may be represented by either of the networks shown in Fig. 5.20, or the simplified versions shown in Fig. 5.21 where

$$\begin{aligned} C'_{E0} &= \frac{-C_{E0}C_{MS}(d^2/E^2C_{MS}^2)}{C_{E0} - C_{MS}(d^2/E^2C_{MS}^2)} = \frac{C_{E0}d^2}{-E^2C_{MS}C_{E0} + d^2} \\ &= \frac{C_{E0}}{1 - (E^2/d^2)C_{MS}C_{E0}} \end{aligned} \tag{5.41}$$

$$C'_{MS} = \frac{C_{MS}}{1 - (E^2/d^2)C_{MS}C_{E0}} \tag{5.42}$$

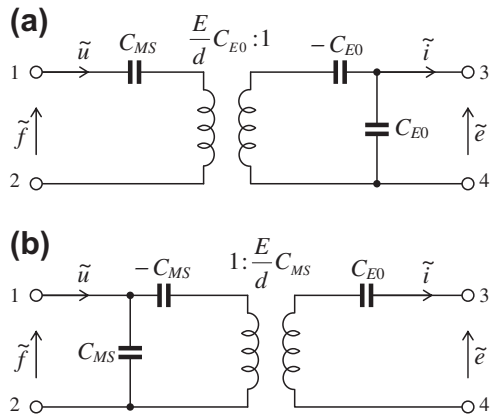

FIG. 5.20 Alternate electromechanical analogous circuits for electrostatic microphones (impedance analogy).

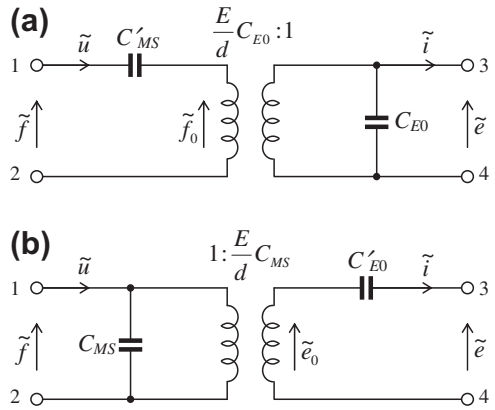

FIG. 5.21 Simplified alternate electromechanical analogous circuits for electrostatic microphones (impedance analogy).

Note in particular that:

C_{E0} is electrical capacitance measured with the mechanical "terminals" blocked so that no motion occurs ($\tilde{u} = 0$).
C'_{E0} is electrical capacitance measured with the mechanical "terminals" operating into zero mechanical impedance so that no force is built up ($\tilde{f} = 0$).
C_{MS} is mechanical compliance measured with the electrical terminals open-circuited ($\tilde{i} = 0$).
C'_{MS} is mechanical compliance measured with the electrical terminals short-circuited ($\tilde{e} = 0$).

The negative elements $-C_{E0}$ and $-C_{MS}$ in Fig. 5.20 (a) and (b) respectively are due to the force of electrostatic attraction towards the back plate. These circuits were first shown as Fig. 3.37 and

Fig. 3.38, and the element sizes were given in Eqs. (3.36) and (3.37). In practice, the circuit of Fig. 5.21b is ordinarily used for electrostatic microphones.

When the microphone shown in Fig. 5.19 is radiating sound into air, the force built up at the face of the microphone when a voltage is applied to electrical terminals (3–4 of Fig. 5.21b) is very small. Hence, when an electric-impedance bridge is used to measure the capacitance of the microphone, the capacitance obtained is approximately equal to C'_{E0}.

By Thévenin's theorem, the capacitor microphone in a free field can be represented by Fig. 5.22. The quantity $\tilde{e}_0$ is the open-circuit voltage produced at the terminals of the microphone by the sound wave and equals [from Eq. (5.40) and Fig. 5.21]

$$\tilde{e}_0 = -\frac{\tilde{u}E}{j\omega d} = -\frac{C_{MS}S\tilde{p}_B E}{d} \tag{5.43}$$

where the force $\tilde{f}_B$, acting on the microphone with the diaphragm blocked so that $\tilde{u} = 0$, is equal to the blocked pressure $\tilde{p}_B$ times the area of the diaphragm S.

Acoustical relations. The microphone of Fig. 5.19 has a diaphragm with the property of mass M_{MD} in addition to the mechanical compliance C_{MS} assumed so far. However, unlike with the dynamic microphone, the two parameters are not separable and it is difficult to evaluate them with any accuracy over the whole frequency range because of the localized nature of the loading on the membrane, which is strongly coupled to the motion of the air in the gap and back-plate openings. However, we will use lumped-parameter elements with approximations in order to gain insight. For the 4190 microphone, the complete acoustical and mechanical circuit in the impedance-type analogy is seen in Fig. 5.23. The internal acoustical circuit consists of an air gap directly behind the diaphragm with an acoustic compliance C_{AG}, a back plate, including holes and a slot, with acoustic resistance and mass R_{AS} and M_{AS}, and a back cavity behind the plate with an acoustic stiffness C_{AB}. The radiation impedance looking outward from the front side of the diaphragm is $R_{AA} + j\omega M_{AA}$, where R_{AA} and M_{AA} are found

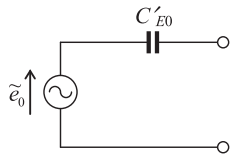

FIG. 5.22 Thévenin's circuit of a capacitor microphone of the type shown in Fig. 5.18 situated in free space.

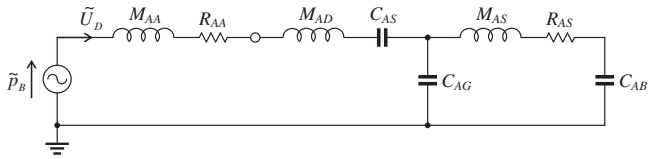

FIG. 5.23 Acoustical circuit of a capacitor microphone including the radiation mass and the acoustical elements behind the diaphragm (impedance analogy).

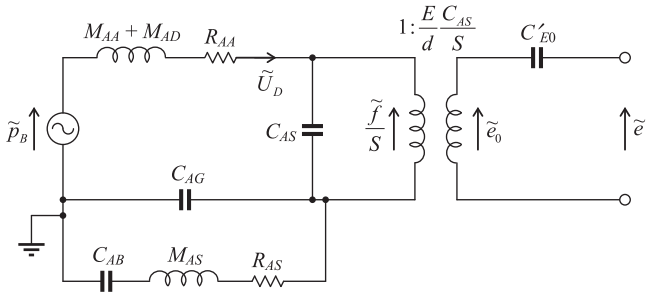

FIG. 5.24 Complete electroacoustical circuit of a capacitor microphone (impedance analogy).

from Table 4.6. In this circuit $\tilde{p}_B$ is the incident pressure at the diaphragm when it is restrained from moving, $M_{AD} = M_{MD}/S^2$ is acoustic mass of the diaphragm, S is effective area of the diaphragm, and $\tilde{U}_D = S\tilde{u}_D$ is volume velocity of the diaphragm.

When Fig. 5.21b is combined with Fig. 5.23, the complete circuit for the electrostatic microphone shown in Fig. 5.24 is obtained.

Performance. The performance of the capacitor microphone shown in Fig. 5.19, viz., the B&K type 4190, can best be understood by reference to Fig. 5.25 and Fig. 5.26, which are derived from Fig. 5.24. At low frequencies the circuit is essentially that of Fig. 5.25*a*. From this circuit, the open-circuit voltage $\tilde{e}_0$ is equal to

$$\tilde{e}_0 = \frac{E}{d}\frac{C_{AB}C_{AS}}{C_{AB} + C_{AS}}\frac{\tilde{p}_B}{S} \tag{5.44}$$

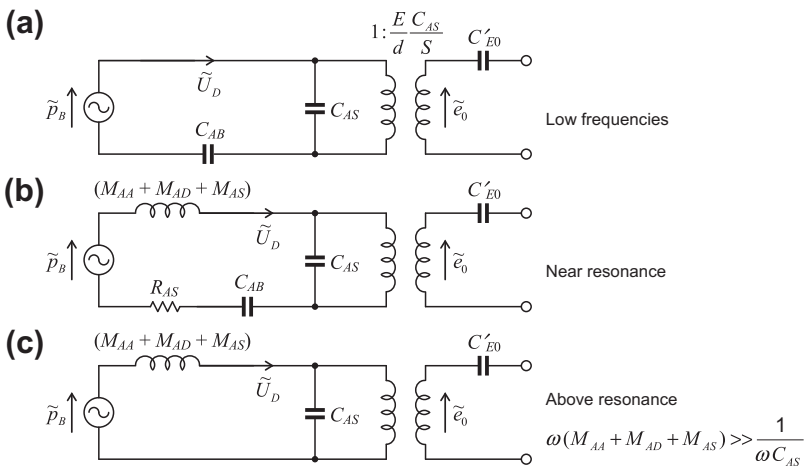

FIG. 5.25 Capacitor microphone—simplified circuits for three frequency regions (impedance analogy).

The excess pressure produced by the sound wave at the diaphragm of the microphone with the microphone held motionless is $\tilde{p}_B$, and the open-circuit voltage is $\tilde{e}_0$.

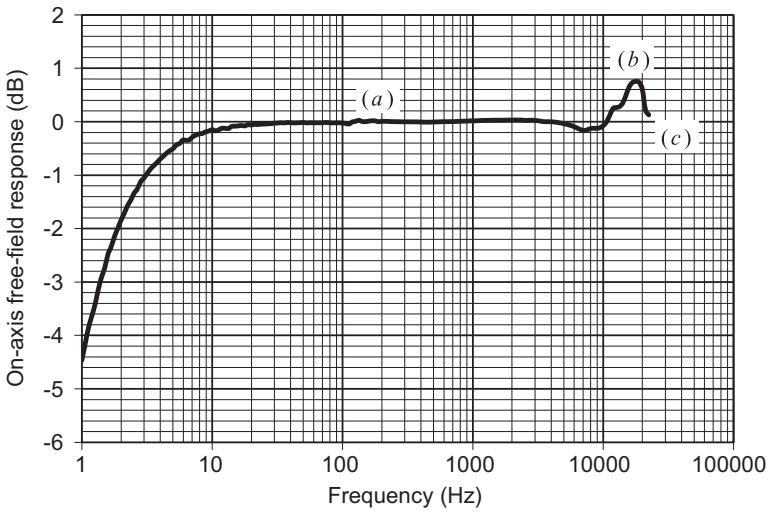

FIG. 5.26 Free-field response of the B&K type 4190 capacitor microphone shown in Fig. 5.19.

Courtesy of Brüel & Kjær Sound & Vibration Measurement A/S.

At low frequencies, therefore, $\tilde{e}_0$ is independent of frequency. This is the frequency region shown as (*a*) in Fig. 5.26. Note that C_{AS} is inversely proportional to the diaphragm tension *T,* and C_{AB} is proportional to the back cavity volume *V* but inversely proportional to the atmospheric pressure P_0 [see Eq. (4.13)]. In a measuring microphone the tension is set high enough so that $C_{AB} >> C_{AS}$ which makes the microphone relatively insensitive to changes in atmospheric pressure.

In the vicinity of the first major resonance, the circuit becomes that of Fig. 5.25b. At resonance, the volume velocity through the compliance C_{AB} is limited only by the magnitude of the acoustic resistance R_{AS}. In general, this resistance is chosen to be large enough so that the resonance peak is less than 2 db (26%) higher than the response at lower frequencies. The response near resonance is shown at (*b*) in Fig. 5.26.

Above the resonance frequency, the circuit becomes that of Fig. 5.25*c*. The volume velocity is controlled entirely by the mass reactance. Hence,

$$\tilde{e}_0 = \frac{E}{\omega^2(M_{AA} + M_{AD} + M_{AS})d}\frac{\tilde{p}_B}{S} \tag{5.45}$$

In this frequency region the response decreases at the rate of 12 dB per octave [see region (*c*) of Fig. 5.26].

At higher frequencies, further resonances could occur, but if they are not completely damped by the radiation resistance R_{AA} (which is no longer negligible compared with $j\omega M_{AA}$), the resonance peaks are likely to be limited by the viscous air flow resistance R_{AS} in the holes or gap.

In a detailed analysis which we shall not reproduce here, Zuckerwar [1] finds that the membrane mass and compliance elements can be approximated by [1]

$$C_{AS} = \frac{S^2}{8\pi T} \tag{5.46}$$

$$M_{AS} = \frac{4\rho_M h}{3S} \tag{5.47}$$

which gives a resonant frequency of

$$\omega_0 = \frac{\sqrt{6}}{a}\sqrt{\frac{T}{\rho_M h}} \tag{5.48}$$

The fundamental resonant frequency of a membrane is

$$\omega_1 = \frac{\alpha_1}{a}\sqrt{\frac{T}{\rho_M h}} \tag{5.49}$$

where $\alpha_1 = 2.4048$ is the first zero of the Bessel function $J_0(x)$. The two frequencies ω_0 and ω_1 differ by only 2%, which implies that the lumped-element model is an accurate representation of the membrane up to ω_0. If we assume the back plate is virtually as large as the membrane, the membrane deflection $\tilde{\eta}(w)$ at low frequencies is given by

$$\tilde{\eta}(w) = \left(1 - \frac{w^2}{a^2}\right)\tilde{\eta}_0 \tag{5.50}$$

where $\tilde{\eta}_0$ is the maximum deflection at the center. Hence the average deflection is given by

$$< \tilde{\eta} > = \frac{2\pi}{S}\int_0^a \tilde{\eta}(w) w dw = \frac{\tilde{\eta}_0}{2} \tag{5.51}$$

Thus the average deflection is half of that at the center, which means that the effective membrane area is half of the total area S. The optimum back plate radius b is given by [1]

$$b = \sqrt{\frac{2}{3}}a \tag{5.52}$$

When designing a capacitor microphone it is desirable to minimize the air gap width d in order to maximize the sensitivity and hence also the signal to noise ratio. Obviously this limits the diaphragm excursion and thus also the maximum sound pressure that can be detected, but this is not generally a problem unless the microphone is designed to record very high sound pressure levels such as those produced by jet engines. Using a small gap, Paschen's law [2] works in our favor because larger electric field strengths (E/d) can be obtained before break down than in larger gaps. Once the gap width and maximum electric field strength has been established, we have to apply enough tension to the membrane in order for it to resist the electrostatic force of attraction towards the back plate. In other words, the positive mechanical compliance C_{MS} in Fig. 5.20a must be less than the negative electrical compliance $-C_{E0}$ when referred to the mechanical side

$$C_{MS} < \frac{d^2}{E^2 C_{E0}} \tag{5.53}$$

However, since $C_{MS} = 1/(8\pi T)$ and $C_{E0} = \varepsilon_0 S/d$ from Eqs. (5.46) and (5.31) respectively, we can write

$$T > \frac{\varepsilon_0 a^2 E^2}{8d^3} \tag{5.54}$$

which is similar to a more rigorous solution [3] based on the static membrane wave equation

$$T > \frac{\varepsilon_0 a^2 E^2}{\alpha_1^2 d^3} \tag{5.55}$$

PART XVII: PRESSURE-GRADIENT MICROPHONES

5.6 ELECTROMAGNETIC RIBBON MICROPHONES

General features. The ribbon microphone has approximately the same sensitivity and impedance as a moving-coil microphone when used with a suitable impedance-matching transformer. Because of its figure 8 directivity pattern it used to be extensively used in broadcast and public-address applications to eliminate unwanted sounds that are situated in space, relative to the microphone, about 90° from those sounds which are wanted, but fell from favor because the delicate ribbon material was too prone to damage. However, since newer more rugged materials have emerged, the ribbon microphone has seen a significant revival of interest in recent years. This has also been helped by the reduction in size and weight made possible by the introduction of neodymium magnets. The ribbon microphone is often preferred by singers to introduce a "throaty" or "bassy" quality into their voices. Similarly, it produces a rich full sound when placed close to amplified instruments. A disadvantage of the ribbon microphone is that, unless elaborate wind screening is resorted to, it is often very noisy when used outdoors.

Construction. A typical form of pressure-gradient microphone is that represented by Fig. 5.27. It consists of a ribbon with a very low resonant frequency hung in a slot in a baffle. A magnetic field transverses the slot so that a movement of the ribbon causes a potential difference to appear across its ends. In this way, the moving conductor also serves as the diaphragm. In modern design, the ribbon element might be 38 mm long, 3.5 mm wide, and 4 μm thick with a clearance of 0.25 mm at each side.

From Eq. (5.11) we see that the pressure difference acting to move the diaphragm is

$$\tilde{p}_R = \tilde{f}_R/S = \tilde{u}\omega\rho_0\Delta l \cos\theta \tag{5.56}$$

where

$\tilde{f}_R$ is net force acting to move the ribbon.
$\tilde{u}$ is particle velocity in the wave in the direction of propagation of the wave.
S is effective area of ribbon.
Δl is effective distance between the two sides.
θ is angle the normal to the ribbon makes with the direction of travel of the wave.

This equation is valid as long as the height of the baffle is less than approximately one-half wavelength.

Analogous circuit. The equivalent circuit (impedance analogy) for this type of microphone is shown in Fig. 5.28. There $\tilde{p}_R$ is the pressure difference which would exist between the two sides of the ribbon

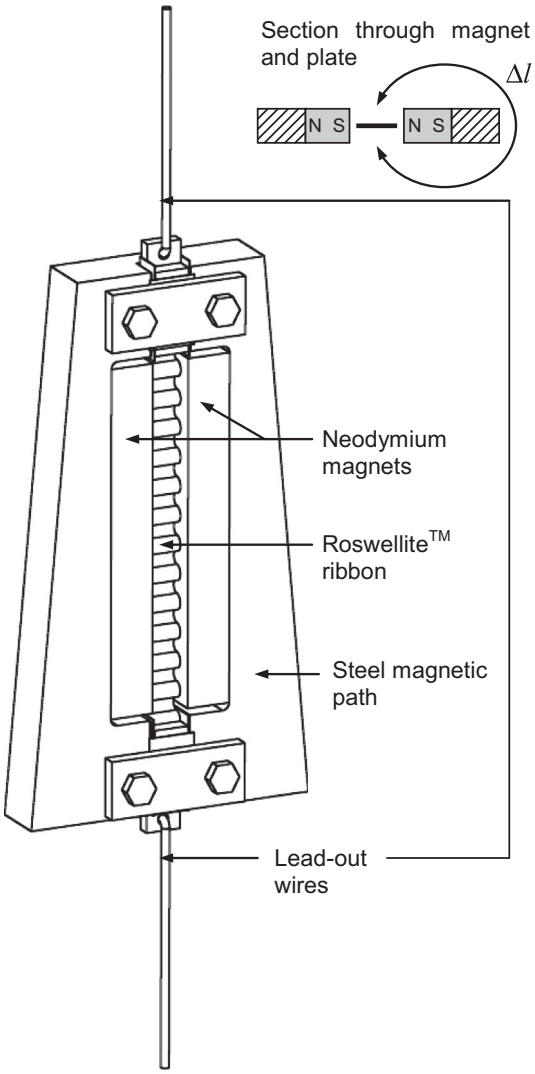

FIG. 5.27 Sketch of the ribbon and magnetic structure for a velocity microphone type KSM313.

The lead-out wires are soldered to metal blocks, and these blocks are clamped against the ribbon by the rectangular plates and the hex-shaped screws which thread into the steel frame.

Courtesy of Shure Incorporated

if it were held rigid and no air could leak around it; Z_{AA} is the acoustic impedance of the medium viewed from one side of the ribbon; $\tilde{U}_R = S\tilde{u}_R$ is volume velocity of the ribbon; $\tilde{u}_R$ is linear velocity of the ribbon; M_{AR}, C_{AR}, and R_{AR} are the acoustic constants of the ribbon itself (for example, $M_{AR} = M_{MR}/S^2$, where M_{MR} is the mass of the ribbon); M_{AS} and R_{AS} are the acoustic mass and resistance, respectively, of the slots at either edge of the ribbon; and $\tilde{U}_S$ is the volume velocity of movement of the air through the slot on the two sides of the ribbon.

Over nearly all the frequency range, the radiation impedance Z_{AA} is a pure mass reactance corresponding to an acoustic mass M_{AA} [see Eq. (4.172)]. In a properly designed microphone, $\tilde{U}_S << \tilde{U}_R$. Also, the microphone is operated above the resonance frequency so that $\omega M_{AR} >> 1/(\omega C_{AR})$. Usually, also, $\omega M_{AR} >> R_{AR}$. Hence, the circuit of Fig. 5.28 simplifies into a single acoustic mass of magnitude $2M_{AA} + M_{AR}$.

When the admittance analogy is used and the electrical circuit is considered, we get the complete circuit of Fig. 5.29. Here, $M_{MA} = M_{AA}S^2$, $M_{MR} = M_{AR}S^2$, B is flux density, l is length of the ribbon, and $\tilde{f}_R = \tilde{p}_R S$.

Performance. The open-circuit voltage $\tilde{e}_0$ of the microphone is found from solution of Fig. 5.29 to be

$$\tilde{e}_0 = \frac{Bl\tilde{f}_R}{j\omega(2M_{MA} + M_{MR})}. \tag{5.57}$$

Substitution of Eq. (5.56) in Eq. (5.57) yields

$$\left|\tilde{e}_0\right| = \left|\tilde{u}\right| \frac{(Bl)\rho_0 \Delta l}{2M_{MA} + M_{MR}} S\cos\theta. \tag{5.58}$$

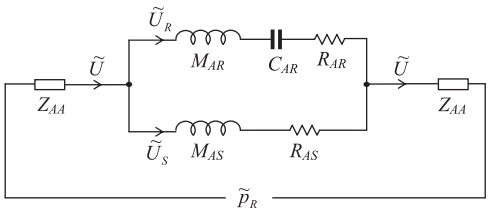

FIG. 5.28 Analogous acoustical circuit for a ribbon microphone (impedance analogy).

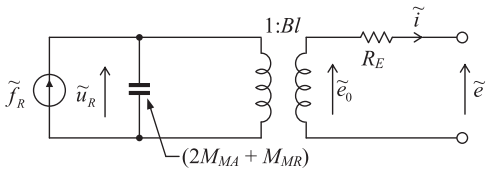

FIG. 5.29 Simplified electromechanical analogous circuit for a ribbon microphone (admittance analogy).

The open-circuit voltage is directly proportional to the component of the particle velocity perpendicular to the plane of the ribbon. In a well-designed ribbon microphone, this relation holds true over the frequency range from 50 to 10,000 Hz. The lower resonance frequency is usually about 15 to 25 Hz. The effects of diffraction begin at frequencies of about 2000 Hz but are counterbalanced by appropriate shaping of the magnetic pole pieces.

PART XVIII: COMBINATION MICROPHONES

5.7 ELECTRICAL COMBINATION OF PRESSURE AND PRESSURE-GRADIENT TRANSDUCERS

One possible way of producing a directivity pattern that has a single maximum (so-called unidirectional characteristic) is to combine electrically the outputs of a pressure and a pressure-gradient microphone. The two units must be located as near to each other in space as possible so that the resulting directional characteristic will be substantially independent of frequency.

Microphones with unidirectional, or cardioid, characteristics are used primarily in broadcast or public-address applications where it is desired to suppress unwanted sounds that are situated, with respect to the microphone, about 180° from wanted sounds. In respect to impedance and sensitivity this type of cardioid microphone is similar to a ribbon or to a moving-coil microphone when suitable impedance-matching transformers are used.

The equation for the magnitude of the open-circuit output voltage of a pressure microphone in the frequency range where its response is "flat" is

$$\tilde{e}_0 = A\tilde{p}. \tag{5.59}$$

The equation for the open-circuit output voltage of a magnetic or ribbon type of pressure-gradient microphone in the same frequency range is

$$\tilde{e}_0' = C\tilde{p}\cos\theta. \tag{5.60}$$

Adding Eq. (5.59) and (5.60) and letting $C/A = B$ gives

$$\tilde{e}_0 = A\tilde{p}(1 + B\cos\theta). \tag{5.61}$$

B will be a real positive number only if $\tilde{e}_0$ and $\tilde{e}_0'$ have the same phase.

The directional characteristic for a microphone obeying Eq. (5.61) will depend on the value of B. For $B = 0$, the microphone is a nondirectional type; for $B = 1$, the microphone is a cardioid type; for $B = \infty$, the microphone is a figure 8 type. The value of B can also take on other values which are optimized for particular characteristics. For example, we may wish to maximize the rejection of ambient or nondirect sound. The directivity factor Q as defined in Eq. (3.142) is given by

$$Q(B) = \frac{2D^2(0)}{\int_0^\pi D^2(\theta)\sin\theta d\theta} = \frac{3(1+B)^2}{3+B^2} \tag{5.62}$$

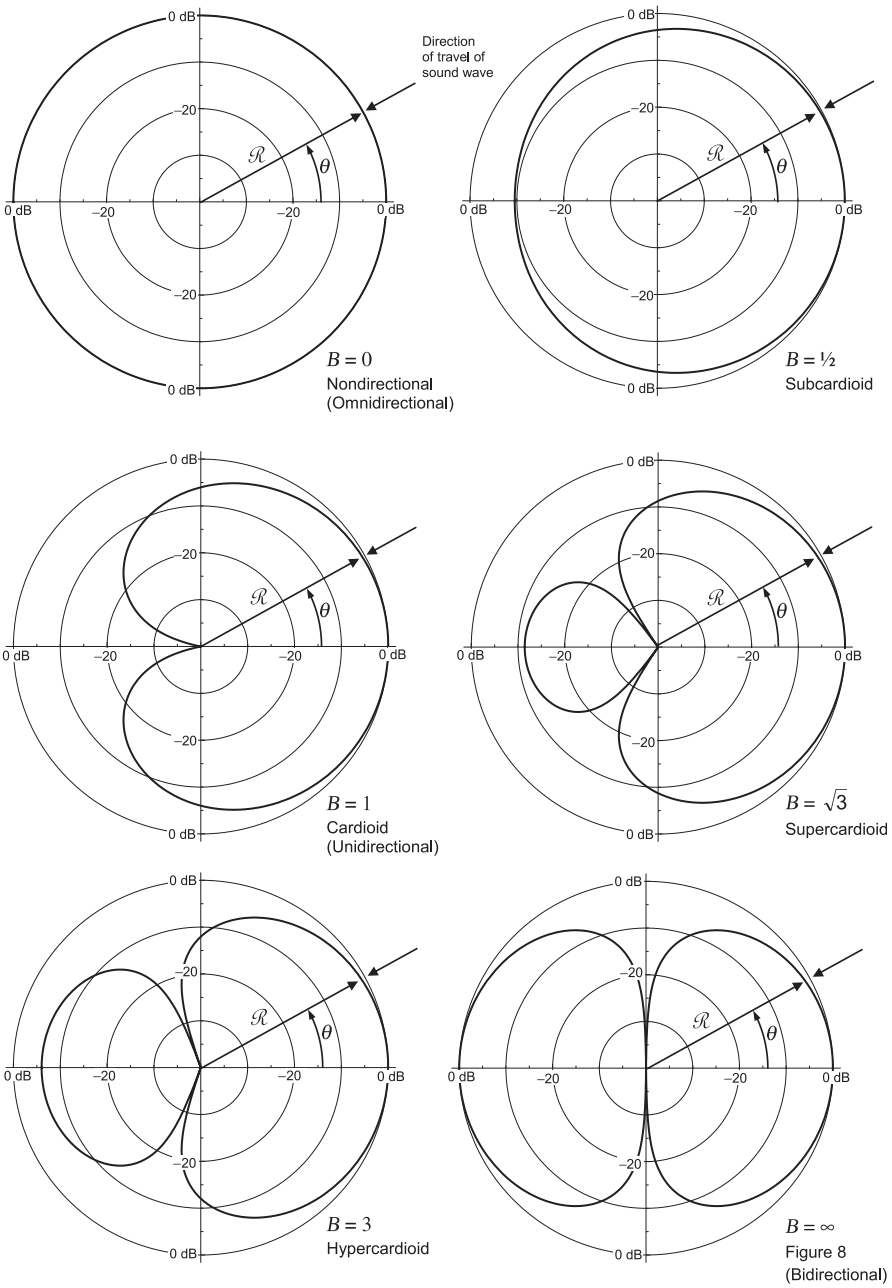

FIG. 5.30 Graphs of the expression $\mathscr{R} = 20 \log_{10}((1 + B\cos\theta)/(1 + B))$ as a function of θ for $B = 0$, ½, 1, $\sqrt{3}$, 3, and ∞.

where the directivity function is given by

$$D(\theta) = \frac{1 + B\cos\theta}{1 + B} \tag{5.63}$$

and on-axis $D(0) = 1$. The condition for maximum off-axis rejection is

$$\frac{\partial}{\partial B} Q(B) = \frac{6(1 + B)(3 - B)}{(3 + B^2)^2} = 0 \tag{5.64}$$

which is met when $B = 3$ and $Q(3) = 4$. This gives what is known as the *hypercardioid* pattern. Alternatively, we may wish to maximize the ratio of the sound captured from the front to that received from the rear, where the rear is defined as anything at an angle of greater than 90°. Let us define the function P such that

$$P(B) = \frac{\int_0^{\pi/2} D^2(\theta)\sin\theta d\theta}{\int_{\pi/2}^{\pi} D^2(\theta)\sin\theta d\theta} = \frac{3 + 3B + B^2}{3 - 3B + B^2} \tag{5.65}$$

The condition for maximum front-to-rear ratio is

$$\frac{\partial}{\partial B} P(B) = \frac{6(3 - B^2)}{(3 - 3B + B^2)^2} = 0 \tag{5.66}$$

which is met when $B = \sqrt{3}$ and $P(\sqrt{3}) = (2 + \sqrt{3})/(2 - \sqrt{3}) = 13.9$. This gives what is known as the *supercardioid* pattern. In Fig. 5.30 directional characteristics for six values of B are shown.

The voltage $\tilde{e}_0'$ is a function of kr, as we discussed in Sec. 5.3, so that the voltage $\tilde{e}_0$ as given by Eq. (5.61) will vary as a function of frequency for small values of $\omega r/c$, where r is the distance between the microphone and a small source of sound. Here, as is the case for a pressure-gradient microphone, a "bassy" quality is imparted to a person's voice if he stands very near the microphone.

5.8. ACOUSTICAL COMBINATION OF PRESSURE AND PRESSURE-GRADIENT MICROPHONES

One example of an acoustical design responding to both pressure and pressure gradient in a sound wave was described earlier in Sec. 5.3 (p. 206). The directional patterns for this type of design are the same as those shown for Fig. 5.30.

In order that this type of microphone has a flat response as a function of frequency for $\tilde{p}$ constant (i.e., constant sound pressure at all frequencies in the sound wave), a transducer must be chosen whose output voltage for a constant differential force acting on the diaphragm is inversely proportional to the quantity A defined in Eq. (5.23), i.e.,

$$\tilde{e}_0 \propto 1/|A| = \left|\frac{Z_{AD} - j[(R_A + Z_{AD})/\omega\, C_A R_A]}{Z_{AD}}\right|. \tag{5.67}$$

As an example, let us take the case of a microphone for which $Z_{AD} >> R_A$ and $1/\omega C_A R_A >> 1$. In this case the response of the transducer must be proportional to

$$1/|A| = \frac{1}{\omega C_A R_A} = \frac{cB}{\Delta l \omega}, \tag{5.68}$$

where B is given by Eq. (5.21).

Restated, the transducer must have an output voltage for a constant net force acting on the diaphragm that is inversely proportional to frequency, if a flat frequency response is desired. This is the case for a moving-coil or ribbon transducer above the natural resonance frequency of the diaphragm.

5.9. DUAL-DIAPHRAGM COMBINATION OF PRESSURE AND PRESSURE-GRADIENT MICROPHONES

A versatile microphone that is popular in recording studios and for recording ensembles on location is the dual-diaphragm variable-pattern capacitor microphone, the schematic of which is shown in Fig. 5.31. It has two diaphragms: one mounted in front (F) of and the other mounted at the back (B) of a common central plate (P). An array of holes in the central plate provides a mixture of resistance and reactance. When the slider of the potentiometer is at position "k", the polarizing voltages on both diaphragms are equal so that they behave like a pair of back-to-back pressure microphones. Hence the resulting directivity pattern is omnidirectional. The low compliance of the air in the holes of the plate ensures that the resonance frequencies of the diaphragms are high in order to provide a suitably wide working bandwidth. As with all pressure microphones, it is stiffness-controlled and displacement-sensitive in this mode.

When the slider is at the other end of its range in position "i", the polarizing voltages on the two diaphragms are of equal magnitude but opposite polarity. Therefore, the microphone is only sensitive to the difference in pressures at the two diaphragms so that they behave more or less as a single diaphragm. Hence the resulting directivity pattern is figure 8. The resonance frequency is now determined by the diaphragm tension instead of the stiffness of the trapped air, which now travels back and forth through the holes providing a high viscous damping resistance. It is this damping resistance which determines the

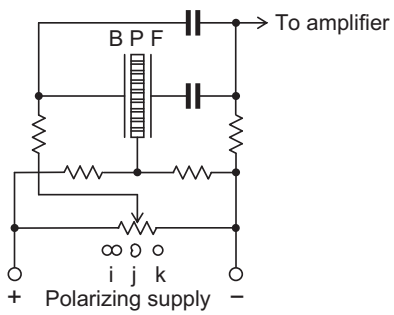

FIG. 5.31 Schematic of a dual-diaphragm capacitor microphone with a variable directivity pattern.

In switch positions "i", "j", and "k", bi-, uni-, and omni-directional directivity patterns are obtained respectively.

bandwidth of the microphone, which is resistance-controlled and velocity-sensitive in this mode. Without this resistance, the frequency response would be just one sharp resonant peak.

When the slider is at position "j", no polarizing voltage is supplied to the diaphragm at the back (B), which in turn no longer contributes to the output voltage. Because it has low mass and high compliance, the back diaphragm is also acoustically transparent so that we have essentially the same configuration as an acoustic combination of pressure and pressure-gradient microphone shown in Fig. 5.7

The analogous circuit for this kind of microphone is shown in Fig. 5.32, where $\tilde{p}_1$ and $\tilde{p}_2$ are the pressures on the outer surfaces of the front and back diaphragms, $\tilde{U}_1$ and $\tilde{U}_2$ are their respective volume velocities, E_1 and E_2 are the front and back polarizing voltages, and $\tilde{e}$ is the microphone output voltage. Also, C_{E0} is the static capacitance of each diaphragm when blocked, $S = \pi a^2$ is the surface area of each diaphragm, d is distance between each diaphragm and the central plate, C_{AP} is the compliance of the air in the holes of the plate, C_{AG} is the compliance of the air in the gap between each diaphragm and the plate, and Z_{AD} is the impedance of each diaphragm which includes the mass, compliance, radiation mass and resistance. The holes in the plate are represented by the T-circuit impedances Z_{AP1} and Z_{AP2} using the tube model shown in Fig. 4.45 except that the holes are assumed to be so narrow that the pressure variations are effectively isothermal and hence R_T can be ignored. The elements C_{E0} and C_{AG} are defined by

$$C_{E0} = \frac{\varepsilon_0 S}{d}, \tag{5.69}$$

$$C_{AG} = \frac{Sd}{\rho_0 c^2}, \tag{5.70}$$

where $\varepsilon_0 = 8.85 \times 10^{-12}$ is the permittivity of free space, $\rho_0 = 1.18$ kg/m^3 is the static density of air, and $c = 345$ m/s is the speed of sound in free space. From Fig. 5.32 we can write the following equations:

$$\tilde{p}_1 = \tilde{p}_a + \left(Z_{AD} + \frac{1}{j\omega C_{AG}}\right)\tilde{U}_1 - \frac{1}{j\omega C_{AG}}\tilde{U}_3, \tag{5.71}$$

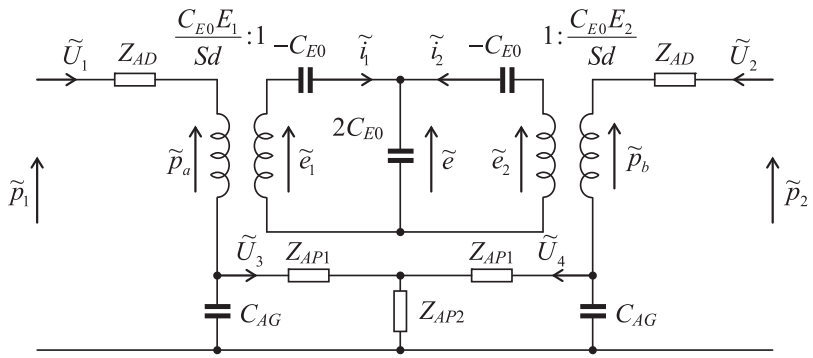

FIG. 5.32 Analogous circuit for a dual-diaphragm capacitor microphone with a variable directivity pattern.

$$\tilde{p}_2 = \tilde{p}_b - \frac{1}{j\omega C_{AG}}\tilde{U}_4 + \left(Z_{AD} + \frac{1}{j\omega C_{AG}}\right)\tilde{U}_2, \tag{5.72}$$

$$0 = -\frac{1}{j\omega C_{AG}}\tilde{U}_1 + \left(Z_{AP1} + Z_{AP2} + \frac{1}{j\omega C_{AG}}\right)\tilde{U}_3 + Z_{AP2}\tilde{U}_4, \tag{5.73}$$

$$0 = -\frac{1}{j\omega C_{AG}}\tilde{U}_2 + Z_{AP2}\tilde{U}_3 + \left(Z_{AP1} + Z_{AP2} + \frac{1}{j\omega C_{AG}}\right)\tilde{U}_4, \tag{5.74}$$

$$\tilde{e}_1 = \frac{Sd}{E_1 C_{E0}}\tilde{p}_a = \left(\frac{1}{-j\omega C_{E0}} + \frac{1}{2j\omega C_{E0}}\right)\tilde{i}_1 + \frac{1}{2j\omega C_{E0}}\tilde{i}_2, \tag{5.75}$$

$$\tilde{e}_2 = \frac{Sd}{E_2 C_{E0}}\tilde{p}_b = \frac{1}{2j\omega C_{E0}}\tilde{i}_1 + \left(\frac{1}{-j\omega C_{E0}} + \frac{1}{2j\omega C_{E0}}\right)\tilde{i}_2, \tag{5.76}$$

$$\tilde{U}_1 = \frac{Sd}{E_1 C_{E0}}\tilde{i}_1, \tag{5.77}$$

$$\tilde{U}_2 = \frac{Sd}{E_2 C_{E0}}\tilde{i}_2, \tag{5.78}$$

$$\tilde{e} = \frac{\tilde{i}_1 + \tilde{i}_2}{2j\omega C_{E0}}. \tag{5.79}$$

Firstly we solve Eqs. (5.73) and (5.74) for $\tilde{U}_3$ and $\tilde{U}_4$ and insert these into Eqs. (5.71) and (5.72). If we then insert $\tilde{p}_a, \tilde{p}_b, \tilde{U}_1$, and $\tilde{U}_2$ from Eqs. (5.75) to (5.78) respectively into Eqs. (5.71) and (5.72), and solve for $\tilde{i}_1$ and $\tilde{i}_2$ before inserting the latter in Eq. (5.79), we obtain an expression for the output voltage $\tilde{e}$. Furthermore, we use the expression for $\tilde{p}_2$ given by Eq. (5.17).

Omni-directional performance

If $E_2 = E_1$, which corresponds to the slider being at position "k" in Fig. 5.31, we have a pressure microphone and the sensitivity is given by

$$\tilde{e}_k = \frac{E_1\left(2 - j\frac{\omega}{c}\Delta l\cos\theta\right)}{2j\omega Sd\left(Z_{AD} + \frac{(Z_{AP1} + 2Z_{AP2})\frac{1}{j\omega C_{AG}}}{Z_{AP1} + 2Z_{AP2} + \frac{1}{j\omega C_{AG}}}\right)}\tilde{p}_1, \tag{5.80}$$

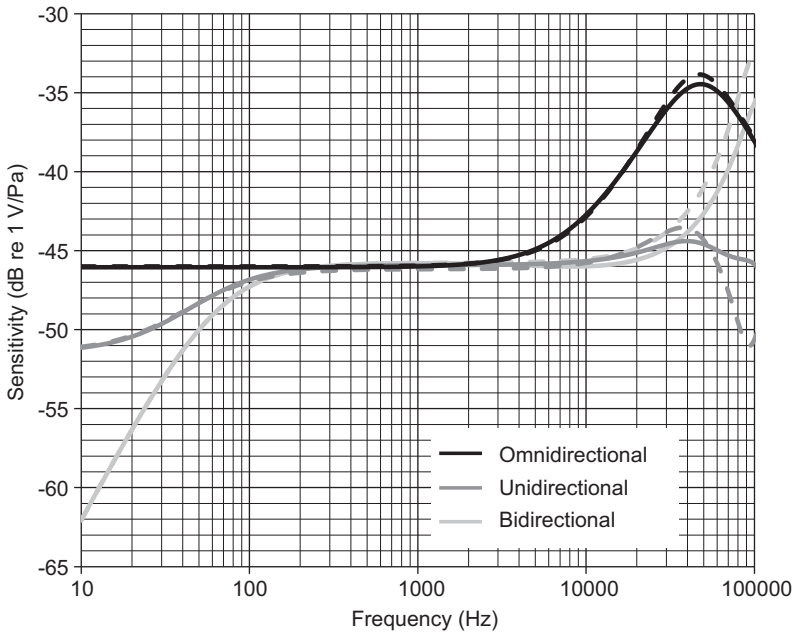

FIG. 5.33 Exact (solid) and approximate (dashed) curves of the on-axis responses of a dual-diaphragm condenser microphone in three different modes: omni-, uni-, and bi-directional.

Exact results from Eqs. (5.80), (5.98), and (5.103) are shown by black, dark gray, and light gray solid curves respectively. Approximate results from Eqs. (5.95), (5.99), and (5.104) are shown by black, dark gray, and light gray dashed curves respectively. The parameters are given in Table 5.2.

where we let

$$\Delta l = l + \pi a/4 \tag{5.81}$$

in accordance with Eq. (5.15) for a resilient disk. Using this formula, the exact on-axis response with the switch in position "i" for an omnidirectional pattern is plotted in Fig. 5.33. We see from this formula that the directivity pattern is essentially omnidirectional provided that

$$f << \frac{c}{3a + \pi l} \tag{5.82}$$

so that the $\cos\theta$ term becomes insignificant. The impedances can be expanded as follows

$$Z_{AD} = j\omega M_{AD} + \frac{1}{j\omega C_{AD}} + \frac{1}{\dfrac{1}{j\omega M_{AR}} + \dfrac{1}{R_{AR}}}, \tag{5.83}$$

$$Z_{AP1} = \frac{R_{AP}}{2} + j\omega\frac{M_{AP}}{2}, \tag{5.84}$$

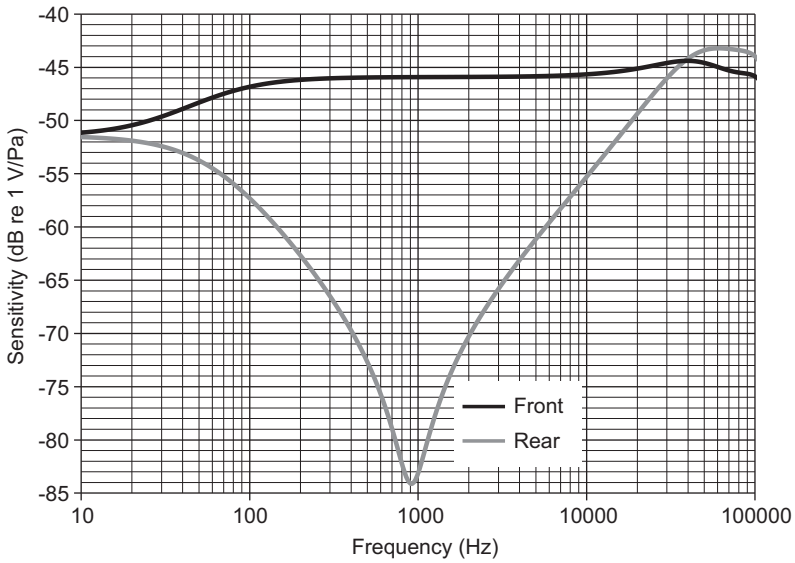

FIG. 5.34 Plots of the on-axis responses at the front (black) and rear (gray) of a dual-diaphragm condenser microphone in unidirectional mode.

The parameters are given in Table 5.2.

$$Z_{AP2} = \frac{1}{j\omega C_{AP}} - \frac{R_{AP}}{6} - j\omega\frac{M_{AP}}{6}, \tag{5.85}$$

where dynamic mass M_{AD} and compliance C_{AD} of the membrane are given by [1]

$$M_{AD} = \frac{4\rho_D h}{3S}, \tag{5.86}$$

$$C_{AD} = \frac{S^2}{8\pi T}, \tag{5.87}$$

where ρ_D is the density of the membrane material, h is its thickness, $S = \pi a^2$ is its surface area, a is its radius, and T is its tension. The acoustic radiation mass and resistance are given by

$$R_{AR} = \frac{\rho_0 c}{S}, \tag{5.88}$$

$$M_{AR} = \frac{\rho_0}{4a}. \tag{5.89}$$

From Chapter 4 the plate mass, compliance and resistance are given by

$$R_{AP} = \frac{8\mu l}{(1+4B_u)a_p^2 S f_f}, \tag{5.90}$$

$$M_{AP} = \frac{1+3B_u}{1+4B_u}\frac{4\rho_0 l}{3Sf_f}, \tag{5.91}$$

$$C_{AP} = \frac{lSf_f}{\rho_0 c^2}, \tag{5.92}$$

where l is the thickness of the plate, a_p is the hole diameter, $\mu = 18.6 \times 10^{-6}$ N·s/m^2 is the viscosity of air, and f_f is the fill factor, which for a rectangular hole grid is given by

$$f_f = \frac{\pi a_p^2}{p^2}, \tag{5.93}$$

where p is the hole pitch. Also B_u is the boundary slip factor which is given by

$$B_u = \left(\frac{2}{\alpha_u} - 1\right)\frac{\lambda_m}{a_p}, \tag{5.94}$$

where $\alpha_u = 0.9$ is the accommodation coefficient and $\lambda_m = 60$ nm is the mean free path length of an air molecule between collisions. It is assumed that the holes are so narrow that the pressure variations within them are isothermal due to heat conduction through the walls. Hence the specific heat ratio γ is absent from the expression for C_{AP}. Because the membrane is flexible as opposed to rigid, the radiation mass M_{AR} is that of a resilient disk in free space as derived in Chapter 13. If we ignore M_{AP}, M_{AR}, R_{AR}, C_{AD}, and ω^3 in Eq. (5.80), we obtain the following approximate formula for the sensitivity

$$\tilde{e}_k \approx \frac{E_1\left(1 - j\frac{\omega}{2c}\Delta l\cos\theta\right)\left(\left(C_{AG} + \frac{C_{AP}}{2}\right) + j\omega\frac{R_{AP}C_{AG}C_{AP}}{12}\right)}{Sd\left(1 - \omega^2 M_{AD}\left(C_{AG} + \frac{C_{AP}}{2}\right) + j\omega\frac{R_{AP}C_{AP}}{12}\right)}\tilde{p}_1. \tag{5.95}$$

Using this formula, the approximate on-axis response with the switch in position "k" for an omnidirectional pattern is plotted in Fig. 5.33 and also in Fig. 533 along with the 180° off-axis response. We see that at low to mid frequencies, where $\omega \to 0$, the reference sensitivity is given by

$$\tilde{e}_{k(\text{ref})} = \frac{E_1\left(C_{AG} + \frac{C_{AP}}{2}\right)}{Sd}\tilde{p}_1. \tag{5.96}$$

The upper limit of the working range is roughly determined by the resonance frequency

$$f_U = \frac{1}{2\pi\sqrt{M_{AD}\left(C_{AG} + \frac{C_{AP}}{2}\right)}}. \tag{5.97}$$

Bi-directional Performance

If $E_2 = -E_1$, which corresponds to the slider being at position "i" in Fig. 5.31, we have a pressure-gradient microphone and the exact sensitivity is given by

$$\tilde{e}_i = \frac{E_1 \Delta l \cos\theta}{2cSd\left(Z_{AD} + \dfrac{Z_{AP1}\dfrac{1}{j\omega C_{AG}}}{Z_{AP1} + \dfrac{1}{j\omega C_{AG}}}\right)} \tilde{p}_1, \tag{5.98}$$

which gives a bidirectional directivity pattern at all frequencies. Using this formula, the on-axis response is plotted in Fig. 5.33 and also in Fig. 5.34 along with the 180° off-axis response. If we ignore M_{AP}, M_{AR} and R_{AR}, we obtain the following approximate formula for the sensitivity

$$\tilde{e}_i \approx \frac{E_1 \Delta l \cos\theta}{2cSd\left(\dfrac{R_{AP}}{2 + j\omega R_{AP} C_{AG}} + j\omega M_{AD} + \dfrac{1}{j\omega C_{AD}}\right)} \tilde{p}_1, \tag{5.99}$$

which is also plotted in Fig. 5.33. We also see that at mid frequencies, where $j\omega C_{AD} > 2/R_{AP}$ but $j\omega M_{AD} < R_{AP}/2$ and $j\omega R_{AP} C_{AG} < 2$, the reference sensitivity is given by

$$\tilde{e}_{i(\text{ref})} = \frac{E_1 \Delta l}{cSdR_{AP}} \tilde{p}_1. \tag{5.100}$$

The lower cut-off frequency is

$$f_L = \frac{1}{\pi R_{AP} C_{AD}} \tag{5.101}$$

and the upper limit of the working range is roughly determined by the resonance frequency:

$$f_U = \frac{1}{2\pi\sqrt{M_{AD} C_{AG}}}. \tag{5.102}$$

Uni-directional Performance

If $E_2 = 0$, which corresponds to the slider being at position "j" in Fig. 5.31, we have a combination pressure and pressure gradient microphone and the exact sensitivity is given by

$$\tilde{e}_j = \frac{\dfrac{1}{2}\left(\tilde{e}_i + \tilde{e}_k\right)}{1 - \dfrac{C_{E0} E_1^2}{4j\omega S^2 d^2}\left\{\left(Z_{AD} + \dfrac{\left(Z_{AP1} + 2Z_{AP2}\right)\dfrac{1}{j\omega C_{AG}}}{Z_{AP1} + 2Z_{AP2} + \dfrac{1}{j\omega C_{AG}}}\right)^{-1} + \left(Z_{AD} + \dfrac{Z_{AP1}\dfrac{1}{j\omega C_{AG}}}{Z_{AP1} + \dfrac{1}{j\omega C_{AG}}}\right)^{-1}\right\}}, \tag{5.103}$$

which is plotted in Fig. 5.33. The expression in the numerator is a pure summation of the pressure and pressure-gradient responses obtained with the switch in positions "k" and "i" respectively. In those positions, all terms containing C_{E0} are balanced out, but in position "j" there is no such balance, which explains the presence of the complicated denominator term in Eq. (5.103). However, the denominator only contributes at low frequencies so that after removing all the high-frequency terms we can make the following approximation:

$$\tilde{e}_j = \frac{\dfrac{2}{R_{AP}C_{AD}} + j\omega}{\dfrac{2}{R_{AP}}\left(\dfrac{1}{C_{AD}} - \dfrac{C_{E0}E_1^2}{4S^2d^2}\right) + j\omega} \cdot \frac{\tilde{e}_i + \tilde{e}_k}{2}, \tag{5.104}$$

which produces a shelf at low frequencies that is determined by the amount of negative stiffness produced by the force of electrostatic attraction. This in fact helps to equalize the amount of low-frequency attenuation, which would otherwise be 6 dB due to taking the half sum of the pressure and pressure-gradient responses, where the former is flat at low frequencies and the latter rolls-off at a rate of 6 dB per octave. The low-frequency shelf starts to rise at the upper frequency of

$$f_{SU} = \frac{1}{\pi R_{AP}C_{AD}} \tag{5.105}$$

and levels off at the lower frequency of

$$f_{SL} = \frac{1}{\pi R_{AP}}\left(\frac{1}{C_{AD}} - \frac{C_{E0}E_1^2}{4S^2d^s}\right). \tag{5.106}$$

The approximate on-axis response with the switch in position "j" for a unidirectional pattern is plotted in Fig. 5.33 where the approximate expressions for $\tilde{e}_i$ and $\tilde{e}_k$ obtained from Eqs. (5.95) and (5.99) respectively are inserted into Eq. (5.104).

Condition for equal sensitivity in all three switch positions

Ideally we would like the sensitivity of the microphone to be the same at all three switch positions "i", "j", and "k". It turns out that this is also the condition for obtaining the optimum cardioid directivity pattern in position "j", which is met by setting $\tilde{e}_i = \tilde{e}_k$ in Eqs. (5.95) and (5.99) in order to yield

$$R_{AP} = \frac{\Delta l}{\left(C_{AG} + \dfrac{C_{AP}}{2}\right)c}, \tag{5.107}$$

which after inserting the path length difference from Eq. (5.15) gives

$$R_{AP} = \frac{l + \dfrac{\pi a}{4}}{\left(C_{AG} + \dfrac{C_{AP}}{2}\right)c}. \tag{5.108}$$

Quite a large resistance is needed to meet this condition so that the holes through the plate have to be very narrow.

Condition for Stability

Another condition which must be met is for the restoring force of the membrane tension to be greater than the force of electrostatic attraction towards the plate. We see from the schematic that this is met if

$$C_{A0} = \left(\frac{Sd}{C_{E0}E_1}\right)^2 C_{E0} > C_{AD} \tag{5.109}$$

or using the expressions from Eqs. (5.69) and (5.87) we obtain the minimum tension value:

$$T > \frac{\varepsilon_0 a^2 E_1^2}{8d^3}. \tag{5.110}$$

Typically the tension should be about three times the minimum value in order to allow for slackening through age and environmental conditions.

Table 5.2 Dual-diaphragm condenser microphone parameters

Membrane		
Radius	a	12.6 mm
Thickness	h	2.5 μm
Density	ρ_D	1400 kg/m^3
Tension	T	50 N/m
Air		
Density	ρ_0	1.18 kg/m^3
Absolute viscosity	μ	17.9 μN·s/m^2
Mean free path	λ	60 nm
Accommodation coefficient	α	0.9
Adiabatic sound speed	c	345 m/s
Specific heat ratio	γ	1.403
Gap	D	50 μm
Permittivity	ε_0	8.85 pF/m
Polarizing voltage	E_1	100 V
Plate		
Hole radius	a_p	6 μm
Hole pitch (center to center)	p	18 μm
Depth	l	1.15 mm

Notes

[1] Zuckerwar AJ. In: Wong GSK, Embleton TFW, editors. AIP Handbook of Condenser Microphones. New York: AIP Press; 1995. p. 47–58. Chap. 3.

[2] Paschen F. Über die zum Funkenübergang in Luft, Wasserstoff und Kohlensäure bei verschiedenen Drucken erforderliche Potentialdifferenz (On the Potential Difference Required to Cause Spark-over in Air, Hydrogen and Carbon Dioxide Under Different Pressures). Ann Phys 1889;273(5):69–75.

[3] Streng JH. Sound radiation from a circular stretched membrane in free space. J. Audio Eng. Soc. 1989;37(3):107–18.